Behavioral/Cognitive

Concurrent- and After-Effects of Medial Temporal Lobe Stimulation on Directed Information Flow to and from Prefrontal and Parietal Cortices during Memory Formation

Anup Das[1] **and Vinod Menon**[1,2,3]

[1]Department of Psychiatry & Behavioral Sciences, [2]Department of Neurology & Neurological Sciences, and [3]Stanford Neurosciences Institute, Stanford University School of Medicine, Stanford, California 94305

Electrical stimulation of the medial temporal lobe (MTL) has the potential to uncover causal circuit mechanisms underlying memory function. However, little is known about how MTL stimulation alters information flow with frontoparietal cortical regions implicated in episodic memory. We used intracranial EEG recordings from humans (14 participants, 10 females) to investigate how MTL stimulation alters directed information flow between MTL and PFC and between MTL and posterior parietal cortex (PPC). Participants performed a verbal episodic memory task during which they were presented with words and asked to recall them after a delay of ~20 s; 50 Hz stimulation was applied to MTL electrodes on selected trials during memory encoding. Directed information flow was examined using phase transfer entropy. Behaviorally, we observed that MTL stimulation reduced memory recall. MTL stimulation decreased top-down PFC→MTL directed information flow during both memory encoding and subsequent memory recall, revealing aftereffects more than 20 s after end of stimulation. Stimulation suppressed top-down PFC→MTL influences to a greater extent than PPC→MTL. Finally, MTL→PFC information flow on stimulation trials was significantly lower for successful, compared with unsuccessful, memory recall; in contrast, MTL→ventral PPC information flow was higher for successful, compared with unsuccessful, memory recall. Together, these results demonstrate that the effects of MTL stimulation are behaviorally, regionally, and directionally specific, that MTL stimulation selectively impairs directional signaling with PFC, and that causal MTL-ventral PPC circuits support successful memory recall. Findings provide new insights into dynamic casual circuits underling episodic memory and their modulation by MTL stimulation.

Key words: **causal circuits in episodic memory; deep brain stimulation; directed information flow; human intracranial EEG; medial temporal lobe; prefrontal and parietal cortices**

Significance Statement

The medial temporal lobe (MTL) and its interactions with prefrontal and parietal cortices (PFC and PPC) play a critical role in human memory. Dysfunctional MTL-PFC and MTL-PPC circuits are prominent in psychiatric and neurologic disorders, including Alzheimer's disease and schizophrenia. Brain stimulation has emerged as a potential mechanism for enhancing memory and cognitive functions, but the underlying neurophysiological mechanisms and dynamic causal circuitry underlying bottom-up and top-down signaling involving the MTL are unknown. Here, we use intracranial EEG recordings to investigate the effects of MTL stimulation on causal signaling in key episodic memory circuits linking the MTL with PFC and PPC. Our findings have implications for translational applications aimed at realizing the promise of brain stimulation-based treatment of memory disorders.

Introduction

The medial temporal lobe (MTL) and its interactions with prefrontal cortex (PFC) play a foundational role in human memory (Vogt and Pandya, 1987; Wagner et al., 2005; Curtis, 2006; Husain and Nachev, 2007; Cabeza et al., 2008; Eichenbaum, 2017; Rolls, 2018, 2019; Rutishauser et al., 2021; Amer and Davachi, 2022). Dysfunctional MTL-PFC circuits are prominent in psychiatric and neurologic disorders, including Alzheimer's disease and schizophrenia (Meyer-Lindenberg et al., 2005; Dickerson and Eichenbaum, 2010; Uhlhaas and Singer, 2012).

Received Sep. 10, 2022; revised Mar. 6, 2023; accepted Mar. 13, 2023.

Author contributions: A.D. and V.M. designed research; A.D. and V.M. performed research; A.D. analyzed data; A.D. wrote the first draft of the paper; A.D. and V.M. edited the paper; A.D. and V.M. wrote the paper.

This work was supported by National Institutes of Health Grants NS086085 and EB022907. We thank Dr. Yuan Zhang for assistance with statistical analysis.

The authors declare no competing financial interests.

Correspondence should be addressed to Anup Das at a1das@stanford.edu or Vinod Menon at menon@stanford.edu.

https://doi.org/10.1523/JNEUROSCI.1728-22.2023

Brain stimulation has emerged as a potential mechanism for enhancing memory function (Fell et al., 2013; J. X. Wang et al., 2014; Ezzyat et al., 2018; Kucewicz et al., 2018b; Alagapan et al., 2019; Yeh and Rose, 2019; van der Plas et al., 2021) and cognitive function (Ramirez-Zamora et al., 2020; Grover et al., 2021), but the underlying neurophysiological mechanisms and dynamic causal circuitry underlying bottom-up and top-down signaling involving the MTL are poorly understood. Given its critical role in memory formation, deep brain stimulation of the MTL with simultaneous recordings in the MTL and PFC has the potential to inform causal circuit mechanisms of encoding and recall in the human brain. Here, we use intracranial EEG (iEEG) recordings to investigate the effects of MTL stimulation on causal signaling in key episodic memory circuits linking the MTL with PFC.

Electrophysiological studies in rodents have reported greater information flow from the MTL to the mPFC than the reverse during spatial working memory (Zhang et al., 2022). In nonhuman primates, MTL-dorsolateral and -ventrolateral PFC interactions have been linked with memory performance (Brincat and Miller, 2015; Cruzado et al., 2020). In humans, fMRI studies have consistently found coactivation of the MTL and multiple PFC regions during both spatial and verbal memory tasks (Dobbins et al., 2002; Simons and Spiers, 2003; Dickerson and Eichenbaum, 2010; Rugg and Vilberg, 2013; Qin et al., 2014; Moscovitch et al., 2016). Moreover, MTL-ventromedial PFC coactivation is also associated with better memory performance (Kumaran et al., 2009). Other studies have shown that functional connectivity between the MTL and mPFC is also associated with memory recall (van Kesteren et al., 2010; Preston and Eichenbaum, 2013; Qin et al., 2014). Furthermore, noninvasive MEG studies in humans have suggested that coherence between the MTL and the superior frontal gyrus and mPFC subdivisions in the delta-theta frequency band is associated with successful memory integration (Guitart-Masip et al., 2013; Backus et al., 2016; Spaak and de Lange, 2020). iEEG studies in humans have reported increased MTL-dorsolateral and -ventrolateral PFC theta band synchronization during episodic memory encoding and recall compared with resting baseline conditions (Anderson et al., 2010; Watrous et al., 2013; Ekstrom and Watrous, 2014; Das and Menon, 2021).

Although prior noninvasive studies have provided significant insights into the role of the MTL and PFC in human episodic memory processing, the causal effects of brain stimulation on the electrophysiology of dynamic "bottom-up" and "top-down" interactions involving the PFC remain unknown. While noninvasive transcranial magnetic stimulation can be used to transiently alter neural processing in targeted cortical regions (J. X. Wang et al., 2014; Yeh and Rose, 2019), it cannot precisely target deep brain structures, such as the MTL (Rossini and Rossi, 2007; Kim et al., 2016). Intracranial electrical stimulation provides an alternative approach that can more precisely map functional brain circuits (Mohan et al., 2020; Paulk et al., 2022) and assess the neurophysiological basis of cognitive processes and its causal basis (Grover et al., 2021; Huang and Keller, 2022; Mercier et al., 2022).

We recently found evidence for asymmetric frequency-specific feedforward and feedback information flow between hippocampus and PFC during memory formation (Das and Menon, 2021). Specifically, we found higher directed information flow from the MTL to the PFC than the reverse, in delta-theta frequency band and higher directed information flow from the PFC to the MTL, than the reverse, in the beta frequency band (Das and Menon, 2021, 2022). Crucially, these findings were observed during both memory encoding and recall periods, indicating a prominent role of delta-theta for "bottom-up" signaling and beta for "top-down" signaling in the cortex.

Here we use iEEG data from the University of Pennsylvania Restoring Active Memory (UPENN-RAM) Consortium (Jacobs et al., 2016; Goyal et al., 2018) to investigate how MTL stimulation alters directed information flow between the MTL and the PFC during episodic memory processing. Participants were presented a list of words during the encoding period and, after a short delay, were asked to recall as many words as possible from the list. During encoding, stimulation was applied at 50 Hz to select MTL electrodes on alternate word pairs, and memory recall was probed after a ~20 s delay period. The choice of 50 Hz stimulation frequency was motivated by its overlap with the gamma band (30-80 Hz), which has been associated with human episodic memory; and the amplitude of iEEG fluctuations in this frequency band has been shown to reflect the underlying activity of single neurons (Kahana, 2006; Lachaux et al., 2012; Kucewicz et al., 2014). Moreover, previous studies have reported that MTL stimulation applied in the 40-50 Hz range has a direct impact on memory performance (Suthana et al., 2012; Fell et al., 2013; Inman et al., 2018). We investigated how MTL stimulation alters its information flow with the PFC. We used phase transfer entropy (PTE) (Lobier et al., 2014; Hillebrand et al., 2016; M. Y. Wang et al., 2017), which provides a robust and powerful measure for characterizing information flow between brain regions based on phase coupling; and crucially, it captures linear as well as nonlinear intermittent and nonstationary dynamics in iEEG data (Menon et al., 1996; Lobier et al., 2014; Hillebrand et al., 2016).

The main goal of our study was to investigate how MTL stimulation alters directed information flow between the MTL and the PFC. We build on our recent findings of asymmetric frequency-dependent directed information flow focused on the delta-theta (0.5-8 Hz) and beta (12-30 Hz) frequency bands (Das and Menon, 2021, 2022). Our analysis focused on the middle frontal gyrus (MFG) encompassing the dorsolateral PFC regions implicated in memory formation and monitoring (Chua and Ahmed, 2016; Rugg, 2022). We contrast this with MTL interactions with the inferior frontal gyrus (IFG) encompassing the ventrolateral PFC regions, which has been implicated in controlled retrieval (Hasegawa et al., 1999; Wagner et al., 2001; Dobbins et al., 2002; Badre et al., 2005; Badre and Wagner, 2007).

The second goal of our study was to determine whether bottom-up and top-down information flow between the MTL and the PFC and posterior parietal cortex (PPC) is similarly impacted by MTL stimulation. Multiple lines of evidence across species have revealed a role for the PPC in episodic memory (Wagner et al., 2005; Cabeza, 2008; Cabeza et al., 2008, 2011, 2012; Hutchinson et al., 2009; Uncapher and Wagner, 2009). Anterograde and retrograde tracing studies in nonhuman primates have uncovered projections from the MTL to the PPC (Clower et al., 2001; Insausti and Muñoz, 2001) and in the reverse direction (Rockland and Van Hoesen, 1999). Single-neuron studies in rodents (Chen et al., 1994; McNaughton et al., 1994; Nitz, 2006) as well as nonhuman primates (Andersen et al., 1985; Crowe et al., 2004) have established PPC involvement in spatial memory. fMRI studies in nonhuman primates have reported coactivation of the MTL and PPC during successful memory encoding and recall (Miyamoto et al., 2013).

Studies using resting-state fMRI in humans have confirmed intrinsic MTL connectivity with the PPC (Vincent et al., 2006). Other human fMRI studies have reported dorsal PPC (dPPC) activation during episodic memory retrieval (Buckner et al.,

1998; Konishi et al., 2000), spatial memory processing (Amorapanth et al., 2010; Baumann et al., 2012), and coactivation of the hippocampus and multiple subdivisions of the PPC during episodic and semantic memory encoding and retrieval (Gurd et al., 2002; Vincent et al., 2006; Ciaramelli et al., 2020). The dPPC is involved in top-down attention processing during memory encoding (Cabeza, 2008; Ciaramelli et al., 2008; Daselaar et al., 2009; Hutchinson et al., 2009; Uncapher and Wagner, 2009; Cabeza et al., 2011, 2012). Human electrocorticography studies have suggested a role for the PPC in verbal episodic memory encoding and recall (Gonzalez et al., 2015), and human iEEG studies have found that hippocampus-PPC correlation in the theta frequency band is prominent in spatial memory (Ekstrom et al., 2005). Together, these findings suggest that coordinated interactions between the MTL and PPC play a role in episodic memory. However, the causal role of MTL-PPC circuits remains poorly understood, and it is not known whether MTL stimulation alters directed information flow between MTL and PPC differently from the PFC.

Our analyses reveal how MTL stimulation alters frequency-specific bottom-up and top-down information flow between the MTL and PFC and how this differs from PPC regions implicated in human episodic memory. Findings provide new insights into causal mechanisms involved in the operation of human episodic memory circuits.

Materials and Methods

UPENN-RAM iEEG recordings. iEEG recordings from 14 patients (10 females, 4 males) shared by Kahana and colleagues at the UPENN (obtained from the UPENN-RAM public data release) were used for analysis (Jacobs et al., 2016; Goyal et al., 2018). Patients with pharmacoresistant epilepsy underwent surgery for removal of their seizure onset zones. iEEG recordings of these patients were downloaded from a UPENN-RAM consortium hosted data sharing archive (URL: http://memory.psych.upenn.edu/RAM). Before data collection, research protocols and ethical guidelines were approved by the Institutional Review Board at the participating hospitals; and informed consent was obtained from the participants and guardians (Jacobs et al., 2016). Details of all the recordings sessions and data preprocessing procedures are described by Kahana and colleagues (Jacobs et al., 2016). Briefly, iEEG recordings were obtained using subdural grids and strips (contacts placed 10 mm apart) or depth electrodes (contacts spaced 5-10 mm apart) using recording systems at each clinical site. iEEG systems included DeltaMed XlTek (Natus), Grass Telefactor, and Nihon-Kohden EEG systems. These patients performed a verbal episodic memory task (see below) and received direct brain stimulation during some of the encoding trials. Electrodes located in brain lesions or those which corresponded to seizure onset zones or had significant interictal spiking or had broken leads, were excluded from analysis.

Anatomical localization of electrode placement was accomplished by coregistering the postoperative computed CTs with the postoperative MRIs using FSL (FMRIB [Functional MRI of the Brain] Software Library), BET (Brain Extraction Tool), and FLIRT (FMRIB Linear Image Registration Tool) software packages. Preoperative MRIs were used when postoperative MRIs were not available. The resulting contact locations were mapped to MNI space using an indirect stereotactic technique and OsiriX Imaging Software DICOM viewer package. We used the Brainnetome atlas (Fan et al., 2016) to demarcate bihemispheric middle and inferior frontal gyrus subdivisions of the prefrontal cortex (MFG and IFG) and dorsal and ventral subdivisions of the posterior parietal cortex (dPPC and vPPC) as well as the hippocampus, parahippocampal gyrus, and entorhinal cortex subdivisions of the MTL. We first identified electrode pairs in patients with electrodes implanted in each pair of brain regions of interest (e.g., MTL-MFG). Key PPC ROIs included the superior parietal lobule, and supramarginal gyrus, intraparietal sulcus, and angular gyrus in the inferior parietal lobule, spanning its dorsal-ventral axis. The lack of sufficient number of participants and electrode pairs precluded analyses of these subdivisions separately. We therefore combined electrodes from the superior parietal lobule, intraparietal sulcus, and supramarginal gyrus into a dPPC subdivision and the angular gyrus regions into a vPPC subdivision (see Tables 2, 3). Ages of these patients ranged from 20 to 49 years, with mean age 36.0 ± 10.1 years, and the dataset included 10 females. Gender differences were not analyzed in this study because of lack of sufficient male participants for electrodes pairs for MTL-MFG, MTL-IFG, MTL-dPPC, and MTL-vPPC interactions (see Table 2).

Original sampling rates of iEEG signals were 500, 1000, and 1600 Hz. Hence, iEEG signals were downsampled to 500 Hz, if the original sampling rate was higher, for all subsequent analysis. The two major concerns when analyzing interactions between closely spaced intracranial electrodes are volume conduction and confounding interactions with the reference electrode (Burke et al., 2013). Hence, bipolar referencing was used to eliminate confounding artifacts and improve the signal-to-noise ratio of the neural signals, consistent with previous studies using UPENN-RAM iEEG data (Burke et al., 2013; Ezzyat et al., 2018). Signals recorded at individual electrodes were converted to a bipolar montage by computing the difference in signal between adjacent electrode pairs on each strip, grid, and depth electrode; and the resulting bipolar signals were treated as new "virtual" electrodes originating from the midpoint between each contact pair, identical to procedures in previous studies using UPENN-RAM data (Solomon et al., 2019). Line noise (60 Hz) and its harmonics were removed from the bipolar signals; and finally, each bipolar signal was Z-normalized by removing mean and scaling by the standard deviation. For filtering, we used a fourth-order two-way zero phase lag Butterworth filter throughout the analysis.

iEEG verbal free recall task and stimulation paradigm. Patients performed multiple trials of a free recall experiment, where they were presented with a list of words and subsequently asked to recall as many as possible from the original list (see Fig. 1*c*) (Solomon et al., 2017, 2019). Each session consisted of 25 lists. The task consisted of three periods: encoding, delay, and recall. During encoding, a list of 12 words was visually presented for ~30 s. Words were selected at random, without replacement, from a pool of high-frequency English nouns (http://memory.psych.upenn.edu/Word_Pools). Each word was presented for a duration of 1600 ms, followed by an interstimulus interval of 800-1200 ms. After a 20 s postencoding delay where participants performed a series of distractor tasks consisting of arithmetic problems of the form $a + b + c = ?$, where a, b, and, c were randomly chosen integers from 1 to 9, participants were instructed to recall as many words as possible during the 30 s recall period.

For each subject, a selected electrode pair in the MTL was connected to an electrical stimulator (Grass Technologies or Blackrock Microsystems) and stimulation was applied using parameters from a prior study (Suthana et al., 2012), showing a positive effect of stimulation on memory performance. Subjects were instructed about the stimulation procedure but were blinded to the location of the stimulation sites. Bipolar-symmetric, charge-balanced, square-wave stimulation current between a pair of electrodes was applied at 50 Hz and 300 μs pulse-width. All the stimulation electrodes in the present study were depth electrodes. Safe amplitude for stimulation was determined at the start of each session under a clinically supervised mapping procedure by manually testing a range of currents for each site, beginning at 0.25 mA and slowly increasing to a maximum of 1.5 mA. The final stimulation current (see Table 1) that was used for the cognitive experiments was the maximum current for each site that could be applied without inducing patient symptoms, epileptiform after discharges, or seizures. We designated a stimulation site being in the MTL if at least one electrode of the bipolar pair was in the region.

For the stimulated lists, exactly half of the words on the list were delivered simultaneously with electrical brain stimulation. For the control lists, all 12 words on the list were presented without stimulation. Out of the 25 lists in each session, 20 were stimulated lists and 5 were control lists in a randomly assigned order. For each stimulated list, stimulation occurred in a blocked pattern: the stimulator was active during the presentation of a pair of consecutive words and then inactive for the

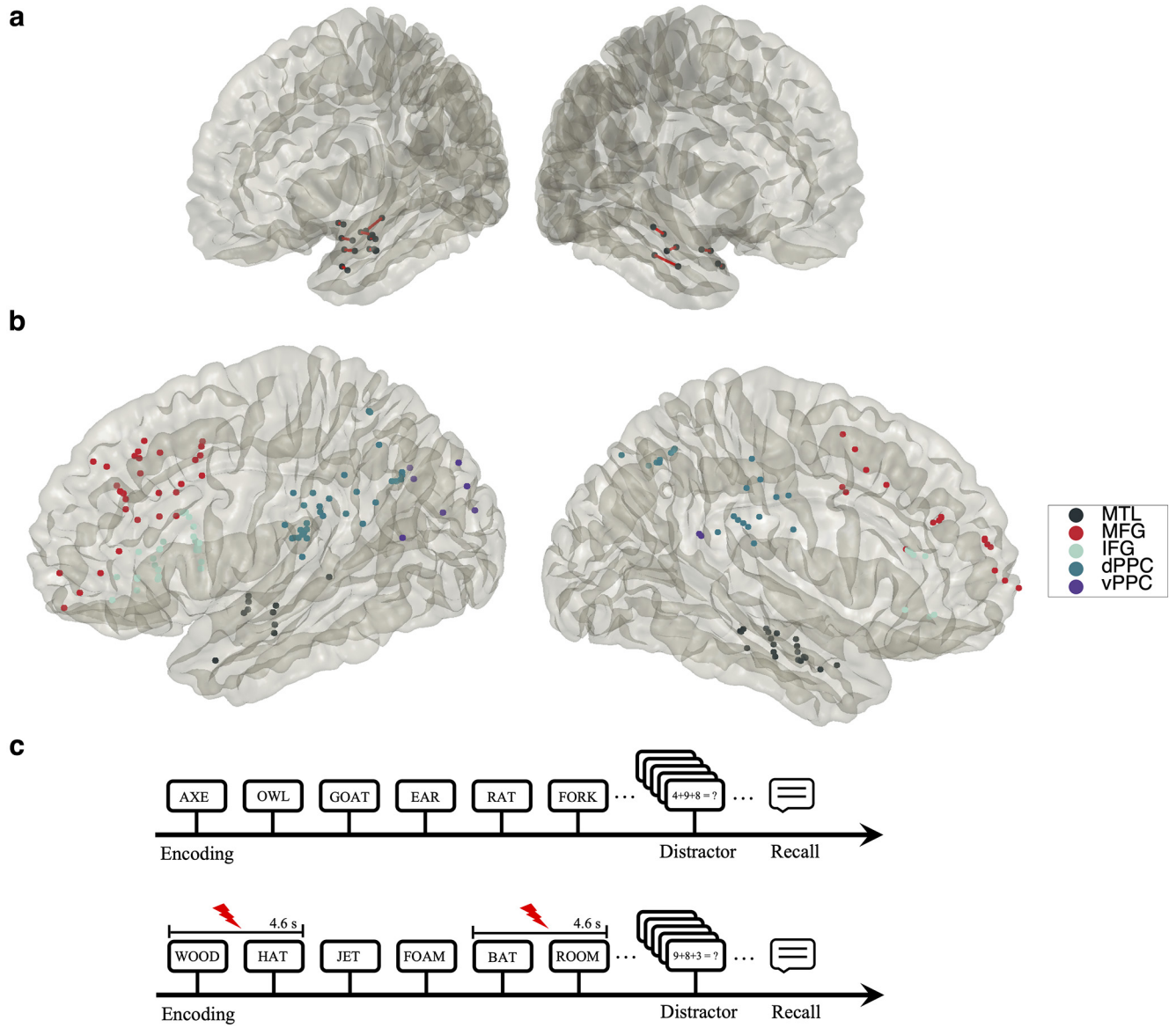

Figure 1. ***a***, Intracranial stimulation sites in the MTL investigated in this study. Each anode-cathode pair of electrodes is connected by a red line. MTL included the hippocampus, parahippocampal gyrus, and entorhinal cortex. ***b***, Nonstimulation iEEG recording sites in the MTL, middle and inferior subdivisions of the PFC (MFG and IFG), and dorsal and ventral subdivisions of the PPC (dPPC and vPPC), investigated in this study. ***c***, Event structure of the verbal episodic memory task during nonstimulation (top) and stimulation (bottom) trials used in this study (for details, see Materials and Methods). Participants were first presented with a list of words in the encoding block and asked to recall as many as possible from the original list after a short delay (distractor period). Stimulation was provided in a blocked pattern; the stimulator was active during the presentation of a pair of consecutive words and then inactive for the following pair. On each stimulated list, the stimulator was active for half the total words (for details, see Materials and Methods).

following pair. Thus, in total, on each stimulated list, the stimulator was active for half the total words. For the stimulation blocks, the stimulator was timed to occur 200 ms before the presentation of the first word in each block, continuing for 4.6 s, until the disappearance of the second word. The onset of stimulation was balanced, such that a random half of the stimulation lists began with a nonstimulated block and the others began with a stimulated block.

We analyzed 1600 ms iEEG epochs from the encoding periods of the free recall task. For the recall periods, iEEG recordings 1600 ms before the vocal onset of each word were analyzed (Solomon et al., 2019). Data from each trial were analyzed separately, and specific measures were averaged across trials. Effects of electrical stimulation on behavioral performance have been analyzed in detail by Kahana and colleagues previously (Jacobs et al., 2016; Goyal et al., 2018). Our major focus in this study was on the effect of stimulation on the direction of information flow between the MTL and the PFC and PPC. The mismatch in the number of trials between successfully versus unsuccessfully encoded words (~1:3) made it difficult to directly compare causal signaling measures associated with the two. From the point of view of probing behaviorally effective memory encoding, our focus was therefore on how MTL stimulation affects successful encoding and recall, consistent with most prior studies (Watrous et al., 2013; Long et al., 2014). For stimulation trials, data corresponding to the pair of words immediately succeeding the stimulated word pair were analyzed. Data corresponding to the stimulated word pair were excluded from analysis to prevent contamination with stimulation artifact (Hansen et al., 2018; Kucewicz et al., 2018b; Jun et al., 2020).

Control analysis using resting-state iEEG data with MTL stimulation. For the control condition, we used "resting-state" data from 2 participants collected in the UPENN-RAM public data release (Solomon et al., 2021). These patients were part of a larger "parameter search" project whose major goal was to systematically study the effects of stimulation frequency, current, and stimulation brain regions (Mohan et al., 2020). We reanalyzed iEEG data from these participants to determine whether

Table 1. Participant demographic information for the memory task and stimulation details (total 14 participants)[a]

Participant ID	Gender	Age	Stimulation electrode type	Stimulation current amplitude (mA)
001	F	48	D	1
003	F	39	D	1.5
020	F	48	D	1.5
030	M	23	D	1
031	M	40	D	1.5
033	F	31	D	1
035	F	45	D	0.5
056	M	34	D	1.5
077	F	47	D	1
085	F	30	D	1.5
101	F	26	D	0.5
111	M	20	D	0.75
112	F	29	D	0.5
150	F	49	D	0.25

[a]D, Depth.

the main findings of directed information flow between the MTL and the PFC and PPC in our study were because of brain stimulation causing reorganization of brain circuits and thus influencing the information flow that we observed in the memory task. Similar to the memory task, bipolar-symmetric, charge-balanced, square-wave stimulation current between a pair of depth MTL electrodes was applied at 50 Hz and 300 μs pulse-width (also see Table 5). Similar procedures were adopted for determining the safe current amplitude for stimulation for these participants. Based on electrode placement in the MTL and the PFC and PPC brain regions and based on the criteria that the stimulation frequency was 50 Hz, we selected 2 subjects with simultaneous electrode placements in MTL and MFG (105 electrode pairs) and also MTL and dPPC (60 electrode pairs). IFG and vPPC were excluded from analysis because of lack of electrode placements in these regions. The stimulation duration for these 2 subjects were 250 and 500 ms (see Table 5).

We analyzed 1600 ms iEEG epochs immediately before the start of each stimulation trial; these correspond to the "non-stim" condition. We also analyzed 1600 ms iEEG epochs immediately after the end of each stimulation trial; these correspond to the "stim" condition. Trials were spaced by 3 s, with up to ±200 ms of randomly applied jitter added to the interval. Subjects were instructed to sit quietly and did not perform any task. Similar to the memory task, data from each trial were analyzed separately and PTE measures were averaged across trials. Data corresponding to the stimulated epochs were excluded from analysis to prevent contamination with stimulation artifact (Hansen et al., 2018; Kucewicz et al., 2018b; Jun et al., 2020).

iEEG analysis of power. For power analysis, we first filtered the signals in the delta-theta (0.5-8 Hz) and beta (12-30 Hz) frequency bands and then calculated the square of the filtered signals as the power of the signals (Kwon et al., 2021). Signals were then smoothed using 0.2 s windows with 90% overlap (Kwon et al., 2021) and normalized with respect to 0.2 s prestimulus periods.

iEEG analysis of PTE and direction of information flow. PTE is a nonlinear measure of the directionality of information flow between time-series and can be applied to nonstationary time-series (Lobier et al., 2014; Das and Menon, 2020). The information flow described here relates to signaling between brain areas and does not necessarily reflect the representation or coding of behaviorally relevant variables per se. The PTE measure is in contrast to the Granger causality measure which can be applied only to stationary time-series (Barnett and Seth, 2014). We first conducted a stationarity test of the iEEG recordings (unit root test for stationarity) (Barnett and Seth, 2014) and found that the spectral radius of the autoregressive model is very close to 1, indicating that the iEEG time-series is nonstationary. This precluded the applicability of the Granger causality analysis in our study.

Given two time-series $\{x_i\}$ and $\{y_i\}$, where $i = 1, 2, \ldots, M$, instantaneous phases were first extracted using the Hilbert transform. Let $\{x_i^p\}$ and $\{y_i^p\}$, where $i = 1, 2, \ldots, M$, denote the corresponding phase time-series. If the uncertainty of the target signal $\{y_i^p\}$ at delay τ is quantified using Shannon entropy, then the PTE from driver signal $\{x_i^p\}$ to target signal $\{y_i^p\}$ can be given by the following:

$$PTE_{x\to y} = \sum_i p\left(y_{i+\tau}^p, y_i^p, x_i^p\right) \log\left(\frac{p\left(y_{i+\tau}^p | y_i^p, x_i^p\right)}{p\left(y_{i+\tau}^p | y_i^p\right)}\right), \quad \text{(i)}$$

where the probabilities can be calculated by building histograms of occurrences of singles, pairs, or triplets of instantaneous phase estimates from the phase time-series (Hillebrand et al., 2016). For our analysis, the number of bins in the histograms was set as $3.49 \times \mathrm{STD} \times \mathrm{M}^{-1/3}$ and delay τ was set as $2\mathrm{M}/\mathrm{M}_{\pm}$, where STD is average standard deviation of the phase time-series $\{x_i^p\}$ and $\{y_i^p\}$ and $\mathrm{M}_{\pm}$ is the number of times the phase changes sign across time and channels (Hillebrand et al., 2016). PTE has been shown to be robust against the choice of the delay τ and the number of bins for forming the histograms (Hillebrand et al., 2016).

iEEG analysis of phase-locking value (PLV) and phase synchronization. We used PLV to compute phase synchronization between two time-series (Lachaux et al., 1999). We first calculated the instantaneous phases of the two signals by using the analytical signal approach based on the Hilbert transform (Bruns, 2004). Given time-series $x(t)$, $t = 1, 2, \ldots, M$, its complex valued analytical signal $z(t)$ can be computed as follows:

$$z(t) = x(t) + i\tilde{x}(t) = A_x(t)e^{\Phi_x(t)}, \quad (1)$$

where i denotes the square root of –1, $\tilde{x}(t)$ is the Hilbert transform of $x(t)$, and $A_x(t)$ and $\Phi_x(t)$ are the instantaneous amplitude and instantaneous phase, respectively, and can be given by the following:

$$A_x(t) = \sqrt{[x(t)]^2 + [\tilde{x}(t)]^2} \text{ and } \Phi_x(t) = \arctan\frac{\tilde{x}(t)}{x(t)}. \quad (2)$$

The Hilbert transform of $x(t)$ was computed as follows:

$$\tilde{x}(t) = \frac{1}{\pi} PV \int_{-x}^{\infty} \frac{x(\tau)}{t-\tau} d\tau, \quad (3)$$

Where *PV* denotes the Cauchy principal value. MATLAB function "hilbert" was used to calculate the Hilbert transform in our analysis. Given two time-series $x(t)$ and $y(t)$, where $t = 1, 2, \ldots, M$, the PLV (zero-lag) can be computed as follows:

$$PLV \triangleq |E[e^{i(\Phi_x(t)-\Phi_y(t))}]|, \quad (4)$$

where $\Phi_y(t)$ is the instantaneous phase for time-series $y(t)$, $|\cdot|$ denotes the absolute value operator, $E[\cdot]$ denotes the expectation operator with respect to time t, and i denotes the square root of –1. PLVs were then averaged across trials to estimate the final PLV for each pair of electrodes.

iEEG analysis of modulation index and phase-amplitude coupling (PAC). We used the modulation index (MI) estimation procedure (Tort et al., 2008) to calculate PAC of electrodes. We first denote the amplitude and the phase frequency ranges for our analysis by f_A ([80, 160] Hz) and fp ([0.5, 8] Hz), respectively. Let $x(t)$ denote the time-series of the electrode. We first filter $x(t)$ at the two frequency ranges f_A and fp. Let us denote the filtered signals as $x_{fA}(t)$ and $x_{fp}(t)$, respectively. We then estimate the phase time-series $\varphi_{fp}(t)$ from the Hilbert transform of $x_{fp}(t)$ and the amplitude time-series $A_{fA}(t)$ from the Hilbert transform of $x_{fA}(t)$. Each point in the composite time-series $[\varphi_{fp}(t), A_{fA}(t)]$ indicates an amplitude of an oscillation in f_A at the corresponding phase in the fp oscillation. We next bin the phases $\varphi_{fp}(t)$ into eighteen 20° intervals (0°-360°) and calculate the mean of A_{fA} over each of the phase bins. Let $\langle A_{fA}\rangle_{\varphi_{fp}}(j)$ denote the mean A_{fA} value at each phase bin j. We then define entropy H as follows:

Table 2. Number of electrode pairs used in the PTE and PLV analysis

Network pairs	No. of electrode pairs (*n*)	No. of participants	Participant IDs (gender/age)
MTL-MFG	132	4	003 (F/39), 020 (F/48), 033 (F/31), 077 (F/47)
MTL-IFG	68	5	003 (F/39), 020 (F/48), 035 (F/45), 077 (F/47), 101 (F/26)
MTL-dPPC	114	8	001 (F/48), 003 (F/39), 020 (F/48), 033 (F/31), 035 (F/45), 077 (F/47), 101 (F/26), 111 (M/20)
MTL-vPPC	23	4	033 (F/31), 077 (F/47), 101 (F/26), 111 (M/20)

Table 3. Number of electrodes in each brain region, used in power and PAC analysis

Brain region	No. of electrodes (*n*)	No. of participants	Participant IDs (gender/age)
MTL	30	10	001 (F/48), 003 (F/39), 020 (F/48), 031 (M/40), 033 (F/31), 035 (F/45), 077 (F/47), 101 (F/26), 111 (M/20), 112 (F/29)
MFG	51	7	003 (F/39), 020 (F/48), 030 (M/23), 033 (F/31), 056 (M/34), 077 (F/47), 085 (F/30)
IFG	35	9	003 (F/39), 020 (F/48), 030 (M/23), 035 (F/45), 056 (M/34), 077 (F/47), 085 (F/30), 101 (F/26), 150 (F/49)
dPPC	52	11	001 (F/48), 003 (F/39), 020 (F/48), 030 (M/23), 033 (F/31), 035 (F/45), 056 (M/34), 077 (F/47), 085 (F/30), 101 (F/26), 111 (M/20)
vPPC	9	4	033 (F/31), 077 (F/47), 101 (F/26), 111 (M/20)

Table 4. Differential effects of stimulation on directed information flow between the MTL and the MFG, IFG, dPPC, and vPPC[a]

Direction	Interaction effect (0.5–8 Hz)	Interaction effect (12–30 Hz)	Stimulation main effect (0.5–8 Hz)	Stimulation main effect (12–30 Hz)
Encode (MTL⟶PFC, PPC)	0.9138971	0.5496000	0.07382400	0.79940000
Encode (PFC, PPC⟶MTL)	0.0025908*	0.5496000	0.00146600	0.41133333
Recall (MTL⟶PFC, PPC)	0.2090900	0.0482400	0.02006667*	0.05436000
Recall (PFC, PPC⟶MTL)	0.9749598	0.0025908*	0.42993429	0.00076512

[a]Results from two-way ANOVA with factors region (MFG, IFG, dPPC, and vPPC) and stimulation (on/off).
*Statistically significant *p* value of interaction, and main effects of stimulation when interactions were nonsignificant (FDR-corrected for multiple comparisons).

Table 5. Participant demographic information for analysis of resting-state iEEG (total 2 participants)[a]

Participant ID	Gender	Age (yr)	Stimulation electrode type	Stimulation current amplitude (mA)	Stimulation duration (ms)
054	M	23	D	1	250
136	F	56	D	2	500

[a]D, Depth.

$$H = -\sum_{j=1}^{N} p_j \log p_j,$$

where $N = 18$ is the number of phase bins and p_j is given by the following:

$$p_j = \frac{\langle A_{fA} \rangle_{\varphi_{fp}}(j)}{\sum_{j=1}^{N} \langle A_{fA} \rangle_{\varphi_{fp}}(j)}.$$

The *MI* is estimated by normalizing H by the maximum possible entropy value H_{max}, which is obtained for the uniform distribution $p_j = 1/N$ ($H_{max} = \log N$) as follows:

$$MI = \frac{H_{max} - H}{H_{max}}.$$

Higher *MI* values indicate stronger PAC, with 0 *MI* corresponding to 0 PAC.

Statistical analysis. Statistical analysis was conducted using mixed effects analysis with the *lmerTest* package (Kuznetsova et al., 2017) implemented in R software (version 4.0.2, R Foundation for Statistical Computing). Because PTE data were not normally distributed, we used BestNormalize (Peterson and Cavanaugh, 2018), which contains a suite of transformation-estimating functions that can be used to optimally normalize data. The resulting normally distributed data were subjected to mixed effects analysis with the following model: *PTE* ~ *Condition* + *(1|Subject)*, where *Condition* models the fixed effects (condition differences) and (1|*Subject*) models the random repeated measurements within the same participant. ANOVA was used to test the significance of findings with false discovery rate (FDR) corrections for multiple comparisons ($p < 0.05$). Analysis of power, PLV, and PAC was conducted in the same manner using the mixed effects analysis.

The differential effects of stimulation on directed information flow between the MTL and the MFG, IFG, dPPC, and vPPC were also tested with a two-way ANOVA with the factors Region (MFG, IFG, dPPC, and vPPC) and Stimulation (ON/OFF). Linear mixed effects analysis was run in a similar way, with the following model: *PTE* ~ *Stimulation* × *Region* + *(1|Subject)*. Two-way ANOVA was then used to test the significance of findings with FDR corrections for multiple comparisons ($p < 0.05$).

For effect size estimation, we used η^2 statistics for complex F-based effects, such as interaction effects and main effects with multiple factors and Cohen's *d* statistics for pairwise *post hoc* comparisons. We used the *eta_squared()* function in the *effectsize* package implemented in R for estimating η^2 and the *lme.dscore()* function in the *EMAtools* package in R for estimating Cohen's *d*.

We also conducted surrogate analysis to test the significance of the estimated PTE values (Hillebrand et al., 2016). The estimated phases from the Hilbert transform for electrodes from a given pair of brain areas were time-shuffled so that the predictability of one time-series from another is destroyed, and PTE analysis was repeated on these shuffled data to build a distribution of surrogate PTE values against which the observed PTE was tested ($p < 0.05$).

Results

Behavioral effects of MTL stimulation

Participants were presented with a sequence of words and asked to remember them for subsequent recall (see Materials and Methods; Tables 1-3; Fig. 1) (Solomon et al., 2019). During encoding, a list of 12 words was visually presented for ~30 s. Each word was presented for a duration of 1600 ms, followed by an interstimulus interval of 800-1200 ms. After a ~20 s

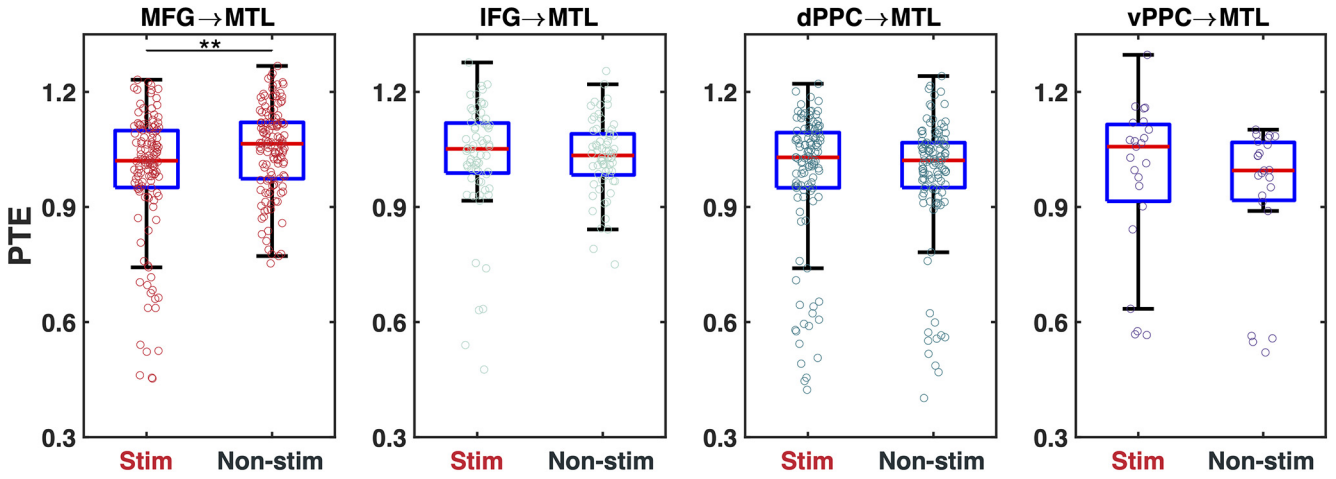

Figure 2. Directed information flow from PFC and PPC to the MTL in δ-theta band (0.5-8 Hz) during stimulation, compared with nonstimulation, trials in the memory encoding period. MFG→MTL information flow, measured using PTE, was reduced during the stimulation, compared with nonstimulation, trials ($n = 132$). In contrast, IFG→MTL ($n = 68$), dPPC→MTL ($n = 114$), and vPPC→MTL ($n = 23$) directed information flow did not differ between stimulation and nonstimulation trials. Central mark indicates the median. Bottom and top edges of the box indicate the 25th and 75th percentiles, respectively. Whiskers extend to the most extreme data points not considered outliers. $^{**}p < 0.01$ (FDR-corrected).

postencoding delay, participants were instructed to recall as many words as possible from the original list during the 30 s recall period. MTL stimulation occurred in a blocked pattern: the stimulator was active during the presentation of a pair of consecutive words and then inactive for the following pair.

Average memory recall accuracy across patients was 22.9 ± 11.7% for MTL stimulation trials and 27.5 ± 12.9% for nonstimulation trials. Memory recall was lower on stimulation, compared with nonstimulation, trials; this difference was marginally significant ($p = 0.0574$, Cohen's $d = 0.51$, Wilcoxon signed-rank test). This result is consistent with prior studies using UPENN-RAM data (Jacobs et al., 2016; Goyal et al., 2018; Kucewicz et al., 2018a) as well as other reports that direct stimulation of the hippocampus generally impairs memory (Halgren et al., 1985; Fernandez et al., 1996; Coleshill et al., 2004; Lacruz et al., 2010; Chua and Ahmed, 2016; Merkow et al., 2017; Herweg et al., 2020; Jun et al., 2020; Jackson et al., 2021).

Effect of MTL stimulation on information flow from MTL to PFC and PPC during memory encoding

We examined the differential effects of stimulation on directed information flow from the MTL to MFG, IFG, dPPC, and vPPC, using a two-way ANOVA with the factors Region (MFG, IFG, dPPC, and vPPC) and Stimulation (ON/OFF) (see Materials and Methods). We focused on directed information flow from the MTL to the PFC and PPC, in the delta-theta and beta bands, based on our replicable findings across verbal and spatial memory domains (Das and Menon, 2021, 2022). To preclude confounding influences associated with unsuccessful recall, we focused on how MTL stimulation affects encoding and recall on successful trials, consistent with prior studies (Watrous et al., 2013; Long et al., 2014). We found no interaction between Stimulation and Region in either delta-theta ($F_{(1,660)} = 0.06$, $p > 0.05$, η^2 = 9.76e-05) or beta ($F_{(1,663)} = 0.68$, $p > 0.05$, η^2 = 1.02e-03) frequency bands during memory encoding. We also did not find any main effects of Stimulation in either delta-theta ($F_{(1,660)} = 3.99$, $p > 0.05$, η^2 = 6.01e-03) or beta ($F_{(1,663)} = 0.06$, $p > 0.05$, η^2 = 9.76e-05) frequency bands during memory encoding (Table 4).

Effect of MTL stimulation on information flow to the MTL from the PFC and PPC during memory encoding

We next examined directed information flow to the MTL from the PFC and PPC during verbal memory encoding. We examined the differential effects of stimulation on directed information flow from the MFG, IFG, dPPC, and vPPC to the MTL, using a two-way ANOVA with factors Region (MFG, IFG, dPPC, and vPPC) and Stimulation (ON/OFF) (see Materials and Methods). We found a significant Stimulation × Region interaction for directed information flow from the PFC and PPC to the MTL in the delta-theta band, ($F_{(1,663)} = 11.75$, $p < 0.01$, η^2 = 0.02) (Table 4). There was no interaction between Stimulation and Region ($F_{(1,663)} = 0.67$, $p > 0.05$, η^2 = 1.01e-03), or main effect of Stimulation ($F_{(1,663)} = 1.04$, $p > 0.05$, η^2 = 1.57e-03) in the beta frequency band (Table 4).

Next, we conducted *post hoc* tests to systematically investigate regional differences in the effects of MTL stimulation on directed information flow to the MTL in the delta-theta band (Fig. 2). MFG→MTL directed information flow decreased during stimulation trials compared with nonstimulation trials in the delta-theta band ($F_{(1,260)} = 12.00$, $p < 0.01$, Cohen's $d = 0.43$) (Fig. 2). In contrast, IFG→MTL ($F_{(1,130)} = 0.42$, $p > 0.05$, Cohen's $d = 0.11$), dPPC→MTL ($F_{(1,220)} = 0.45$, $p > 0.05$, Cohen's d = 0.09), and vPPC→MTL ($F(1,42) = 3.36$, $p > 0.05$, Cohen's d = 0.57) directed information flow did not differ between stimulation and nonstimulation trials. We then compared the strength of top-down information flow to the MTL from the MFG, and dPPC and vPPC, associated with MTL stimulation. MFG→MTL directed information flow did not differ from dPPC→MTL ($F_{(1,28)} = 0.03$, $p > 0.05$, Cohen's $d = 0.07$) and vPPC→MTL ($F_{(1,137)} = 0.17$, $p > 0.05$, Cohen's $d = 0.07$) directed information flow on stimulation trials.

These results demonstrate that MTL stimulation reduces top-down MFG→MTL information flow in the delta-theta band during memory encoding, and that this effect is specific to PFC with no differences in either the dorsal or ventral PPC.

Effect of MTL stimulation on information flow from MTL to PFC and PPC during memory recall

We next examined the differential effects of stimulation on directed information flow from the MTL to the MFG, IFG,

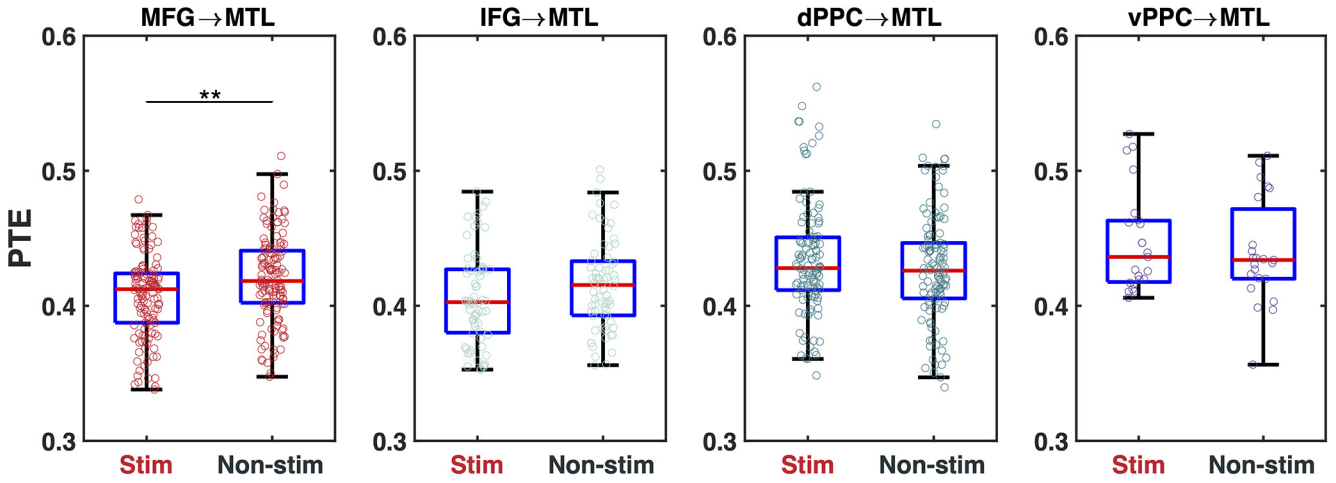

Figure 3. Directed information flow from the PFC and PPC to the MTL in beta band (12-30 Hz) during stimulation, compared with nonstimulation, trials in the memory recall period. MFG→MTL information flow was reduced during the stimulation trials, compared with the nonstimulation trials ($n = 132$). In contrast, IFG→MTL ($n = 68$), dPPC→MTL ($n = 114$), and vPPC→MTL ($n = 23$) directed information flow did not differ between stimulation and nonstimulation trials. $^{**}p < 0.01$ (FDR-corrected).

dPPC, and vPPC, with a two-way ANOVA with the factors Region (MFG, IFG, dPPC, and vPPC) and Stimulation (ON/OFF) during the memory recall period, which occurred ~20 s after word encoding (see Materials and Methods). There was no significant Stimulation × Region interaction in the delta-theta band ($F_{(1,662)} = 2.64$, $p > 0.05$, $\eta^2 = 3.98\text{e-}03$) (Table 4). However, there was a main effect of Stimulation, with higher directed information flow from the MTL to the PFC and PPC during trials with stimulation ($F_{(1,662)} = 7.19$, $p < 0.05$, $\eta^2 = 0.01$). There was no Stimulation × Region interaction ($F_{(1,663)} = 5.61$, $p = 0.05$, $\eta^2 = 8.39\text{e-}03$) or main effect of Stimulation ($F_{(1,663)} = 4.62$, $p > 0.05$, $\eta^2 = 6.91\text{e-}03$) in the beta band (Table 4).

Effect of MTL stimulation on information flow to MTL from PFC and PPC during memory recall

We next examined the differential effects of stimulation on directed information flow from the MFG, IFG, dPPC, and vPPC to the MTL, with a two-way ANOVA with the factors Region (MFG, IFG, dPPC, and vPPC) and Stimulation (ON/OFF) during the memory recall period (see Materials and Methods). In the delta-theta band, we found no significant Stimulation × Region interaction ($F_{(1,663)} = 0.00$, $p > 0.05$, $\eta^2 = 1.49\text{e-}06$) or main effect of Stimulation ($_{F(1,663)} = 0.78$, $p > 0.05$, $\eta^2 = 1.18\text{e-}03$) (Table 4).

We found a significant Stimulation × Region interaction for directed information flow from PFC and PPC to MTL in the beta band ($F_{(1,663)} = 11.92$, $p < 0.01$, $\eta^2 = 0.02$) (Table 4). *Post hoc* analysis of this interaction revealed that MFG→MTL directed information flow decreased during stimulation, compared with the nonstimulation, trials ($F_{(1,260)} = 11.11$, $p < 0.01$, Cohen's $d = 0.41$) (Fig. 3). In contrast, IFG→MTL ($F_{(1,130)} = 3.75$, $p > 0.05$, Cohen's $d = 0.34$), dPPC→MTL ($F_{(1,220)} = 1.93$, $p > 0.05$, Cohen's $d = 0.19$), and vPPC→MTL ($F_{(1,41)} = 0.48$, $p > 0.05$, Cohen's $d = 0.22$) information flow did not differ between stimulation and nonstimulation trials. We then compared the strength of top-down information flow to the MTL from the MFG and dPPC associated with MTL stimulation. This analysis revealed that MFG→MTL directed information flow was significantly lower than dPPC→MTL information flow on stimulation trials ($F_{(1,213)} = 10.02$, $p < 0.01$, Cohen's $d = 0.43$) (Fig. 4). MFG→MTL directed information flow did not differ from dPPC→MTL information flow during nonstimulation trials ($F_{(1,104)} = 3.50$, $p > 0.05$, Cohen's $d = 0.37$). MFG→MTL directed information flow was lower than vPPC→MTL information flow during both stimulation ($F_{(1,149)} = 17.23$, $p < 0.001$, Cohen's $d = 0.68$) (Fig. 4) and nonstimulation trials ($F_{(1,142)} = 10.26$, $p < 0.01$, Cohen's $d = 0.56$).

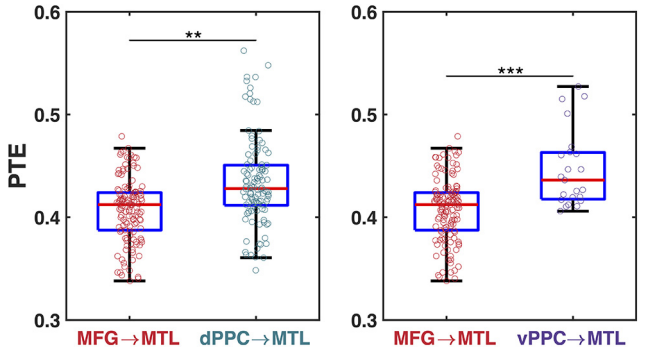

Figure 4. Comparison of directed information flow from the MFG and dPPC/vPPC to the MTL in beta band (12-30 Hz) during stimulation trials in the memory recall period. MFG→MTL ($n = 132$) information flow was significantly lower during the stimulation trials compared with both dPPC→MTL ($n = 114$) and vPPC→MTL ($n = 23$) information flow. $^{***}p < 0.001$; $^{**}p < 0.01$; FDR-corrected.

Together, these results suggest that MTL stimulation reduces top-down directed information flow from the MFG subdivision of the PFC to the MTL in the beta band during memory recall. Results further suggest that MTL stimulation selectively suppresses top-down influences from the MFG, compared with both dorsal and ventral PPC, and that the PFC is relatively more sensitive to the effects of stimulation compared with the PPC.

Effect of MTL stimulation on information flow between the MTL and the PFC and PPC in resting state

To determine whether our main findings related to the direction of information flow between the MTL and the PFC and PPC in our study were specific to the effects of memory processing, we used "resting-state" data from participants collected in the UPENN-RAM public data release (Solomon et al., 2021). Subjects were instructed to sit quietly and did not perform any task. Similar to the memory task, bipolar stimulation current between pairs of depth MTL electrodes was applied at 50 Hz (Table 5). Based on electrode placement in the MTL and the

PFC and PPC brain regions and based on the criteria that the stimulation frequency was 50 Hz, we selected 2 subjects ($n = 105$ electrode pairs for MFG and $n = 60$ electrode pairs for dPPC; IFG and vPPC did not have electrode sampling) with simultaneous electrode placements in MTL and MFG and also MTL and dPPC. We analyzed 1600 ms iEEG epochs immediately before the start of each stimulation trial; these correspond to the "non-stim" condition. We also analyzed 1600 ms iEEG epochs immediately after the end of each stimulation trial; these correspond to the "stim" condition.

We found that, in contrast to the memory task, neither MTL→MFG ($F_{(1,207)} = 0.04$, $p > 0.05$, Cohen's $d = 0.03$) nor MFG→MTL ($F_{(1,207)} = 0.00$, $p > 0.05$, Cohen's $d = 0.00$) directed information flow changed during stimulation, compared with the nonstimulation, trials in the delta-theta frequency band. Moreover, neither MTL→MFG ($F_{(1,207)} = 1.44$, $p > 0.05$, Cohen's $d = 0.17$) nor MFG→MTL ($F_{(1,207)} = 3.35$, $p > 0.05$, Cohen's $d = 0.25$) directed information flow changed during stimulation, compared with the nonstimulation, trials in the beta frequency band.

Furthermore, we found that neither MTL→dPPC nor dPPC→MTL directed information flow changed during stimulation, compared with the nonstimulation, trials in both the delta-theta ($F_{(1,117)} = 1.69$, $p > 0.05$, Cohen's $d = 0.24$ for MTL→dPPC and $F_{(1,117)} = 0.08$, $p > 0.05$, Cohen's $d = 0.05$ for dPPC→MTL) and beta ($F_{(1,117)} = 0.01$, $p > 0.05$, Cohen's $d = 0.02$ for MTL→dPPC and $F_{(1,117)} = 0.84$, $p > 0.05$, Cohen's $d = 0.17$ for dPPC→MTL) frequency bands.

Together, these results suggest that the reported results related to direction of information flow between the MTL and the PFC and PPC, which we observed during the memory task, cannot be solely attributable to effects of brain stimulation causing reorganization of brain circuits; rather, they are related to the combined effects of stimulation and memory processing.

Comparison of information flow between the MTL and the PFC and PPC during memory processing and resting state

To provide further evidence that our main findings related to the direction of information flow between the MTL and the PFC and PPC were specific to the effects of memory processing, we directly compared information flow from the MTL to the PFC and PPC, and the reverse, for the memory encoding and recall conditions with the resting-state condition, during the stimulation trials.

We first focused our analysis on bottom-up directed information flow from the MTL to the PFC and PPC. This analysis revealed that MTL→MFG directed information flow was higher for both memory encoding ($F_{(1,235)} = 8.34$, $p < 0.01$, Cohen's $d = 0.38$) and recall ($F_{(1,115)} = 23.72$, $p < 0.001$, Cohen's $d = 0.91$) compared with rest, during stimulation in the delta-theta frequency band. This finding was reversed in the beta frequency band, where MTL→MFG directed information flow was lower for both memory encoding ($F_{(1,233)} = 16.33$, $p < 0.001$, Cohen's $d = 0.53$) and recall ($F_{(1,233)} = 36.70$, $p < 0.001$, Cohen's $d = 0.79$) compared with rest. MTL→dPPC directed information flow was higher for both memory encoding ($F_{(1,170)} = 29.73$, $p < 0.001$, Cohen's $d = 0.83$) and recall ($F_{(1,161)} = 39.08$, $p < 0.001$, Cohen's $d = 0.99$) compared with rest, during stimulation in the delta-theta frequency band. MTL→dPPC directed information flow was also higher for memory recall ($F_{(1,169)} = 5.75$, $p < 0.05$, Cohen's $d = 0.37$) compared with rest, during stimulation in the beta band; however, MTL→dPPC directed information flow did not differ for memory encoding and rest conditions in the beta band ($F_{(1,170)} = 0.08$, $p > 0.05$, Cohen's $d = 0.04$). These results suggest that the "bottom-up" effects of stimulation on memory processing enhance MTL to PFC information flow in the delta-theta frequency band and suppress this information flow in the beta frequency band, compared with rest. On the other hand, the "bottom-up" effects of stimulation on memory processing enhance MTL to PPC information flow in both delta-theta and beta frequency bands, compared with rest.

We next examined top-down directed information flow from the PFC and PPC to the MTL. This analysis revealed that MFG→MTL directed information flow was lower for both memory encoding ($F_{(1,172)} = 42.28$, $p < 0.001$, Cohen's $d = 0.99$) and recall ($F_{(1,181)} = 35.23$, $p < 0.001$, Cohen's $d = 0.88$) compared with rest, in the delta-theta frequency band and for memory recall compared with rest, in the beta frequency band ($F_{(1,235)} = 47.55$, $p < 0.001$, Cohen's $d = 0.90$). MFG→MTL directed information flow did not differ between memory encoding and rest in the beta band ($F_{(1,235)} = 0.05$, $p > 0.05$, Cohen's $d = 0.03$). dPPC→MTL directed information flow was lower for both memory encoding ($F_{(1,21)} = 15.00$, $p < 0.01$, Cohen's $d = 1.67$) and recall ($F_{(1,172)} = 14.26$, $p < 0.001$, Cohen's $d = 0.58$) compared with rest, in the delta-theta frequency band. dPPC→MTL directed information flow was higher for memory encoding ($F_{(1,161)} = 15.46$, $p < 0.001$, Cohen's $d = 0.62$), but lower for memory recall ($F_{(1,172)} = 13.41$, $p < 0.001$, Cohen's $d = 0.56$) compared with rest, during stimulation in the beta band. These results suggest that the "top-down" effects of stimulation on memory processing mostly suppress information flow from the PFC and PPC to the MTL compared with rest.

Together, these results provide further evidence that the reported results related to direction of information flow between the MTL and the PFC and PPC, during the memory task, cannot be solely attributable to effects of brain stimulation causing reorganization of brain circuits. Rather, they are related to the combined effects of stimulation and memory processing.

Effect of MTL stimulation on directed information flow for successful versus unsuccessful memory recall

We next examine the effect of stimulation on directed information flow for successful compared with unsuccessful memory trials. To directly examine behavioral effects of stimulation, we focus our results on the memory recall periods (for results related to the memory encoding periods where strong behavioral signatures were absent, see Table 6). This analysis revealed that MTL→MFG directed information flow was significantly lower for successful, compared with unsuccessful, memory recall in the beta band ($F_{(1,259)} = 18.50$, $p < 0.001$, Cohen's $d = 0.53$) (Fig. 5). MTL→vPPC directed information flow was significantly higher for successful, compared with unsuccessful, memory recall in both delta-theta ($F_{(1,41)} = 24.01$, $p < 0.001$, Cohen's $d = 1.62$) and beta ($F_{(1,41)} = 10.27$, $p < 0.01$, Cohen's $d = 0.77$) frequency bands (Fig. 5).

Together, these results suggest that the strongest behavioral effects of MTL stimulation are in the bottom-up direction, mediating information flow from MTL to MFG and vPPC. Results also suggest that both stimulation and memory processing contribute to directed information flow between the MTL and the PFC and PPC that we observed during the memory task.

Surrogate data analysis of directed information flow between the MTL and the PFC and PPC

Next, we conducted surrogate data analysis to test the significance of the estimated PTE values compared with PTE expected by chance (see Materials and Methods) for the stimulation trials.

Table 6. Differential effects of MTL stimulation on directed information flow for successful versus unsuccessful memory during encoding and recall periods

Direction	0.5–8 Hz	12–30 Hz
Memory encoding		
MTL⟶MFG	0.0252080	0.9950
MTL⟶IFG	0.9338286	0.9950
MTL⟶dPPC	0.0252080	0.9950
MTL⟶vPPC	0.9338286	0.9950
MFG⟶MTL	0.9338286	0.8712
IFG⟶MTL	0.9958000	0.9950
dPPC⟶MTL	0.9338286	0.9950
vPPC⟶MTL	0.9338286	0.9950
Memory recall		
MTL⟶MFG	0.29573333	0.00017304*
MTL⟶IFG	0.09964000	0.50540000
MTL⟶dPPC	0.44040000	0.04010667
MTL⟶vPPC	0.00012136*	0.00869200*
MFG⟶MTL	0.50053333	0.32848000
IFG⟶MTL	0.50053333	0.39906667
dPPC⟶MTL	0.68120000	0.32848000
vPPC⟶MTL	0.68120000	0.50540000

*Statistically significant p value (FDR-corrected for multiple comparisons).

The estimated phases from the Hilbert transform for electrodes from pairs of brain areas were time-shuffled, and PTE analysis was repeated on these shuffled data to build a distribution of surrogate PTE values against which the observed PTE was tested.

Surrogate data analysis revealed that directed information flow from the MTL to MFG, IFG, dPPC, and vPPC and in the reverse direction was significantly higher than that expected by chance ($p < 0.05$ in all cases) in the delta-theta frequency band during both memory encoding and recall periods. In contrast, in the beta frequency band, directed information flow from the MTL to PFC and PPC subdivisions, and in the reverse direction, was significantly lower than that expected by chance ($p < 0.05$ in all cases) during both memory encoding and recall periods.

These results demonstrate that the reported directed information flow between different brain areas during stimulation trials arises from causal signaling that is enhanced significantly above chance levels.

Effects of MTL stimulation on intraregional information flow

Next, we examined information flow between electrode pairs within each of the individual brain regions examined above. We found that information flow between the electrodes did not differ between the stimulation and nonstimulation trials in any of the brain regions examined (MTL, MFG, dPPC, vPPC) during either memory encoding or recall in the delta-theta or beta bands (p values > 0.05, Cohen's $d < 1.16$). However, information flow in the IFG was higher for stimulation, compared with nonstimulation, trials in the beta band during memory recall ($F_{(1,60)} = 9.45$, $p < 0.05$, Cohen's $d = 0.79$). These results indicate that MTL stimulation has minimal effect on intraregional directed information flow.

Effects of MTL stimulation on phase synchronization between MTL and PFC and PPC

In addition to analysis of time-delayed directed information flow using PTE, we also examined instantaneous phase synchronization between the MTL and the PFC and PPC. Analysis of instantaneous PLVs (see Materials and Methods) revealed that phase-locking of the MTL with the MFG, IFG, dPPC, vPPC did not differ between stimulation and nonstimulation trials for either memory encoding or recall in the delta-theta or beta bands (p values > 0.05, Cohen's $d < 0.70$). These results suggest that the neuromodulatory effects of MTL stimulation are a consequence of the time-delayed interactions between different brain areas as precisely captured by the PTE measure rather than instantaneous synchronization measures such as the PLV.

Effects of MTL stimulation on intraregional phase synchronization

Next, we used PLV to examine information flow between electrodes pairs within each of the individual brain regions. We found that phase-locking between the electrodes did not differ between stimulation and nonstimulation trials in any of the brain regions during both memory encoding and recall, in the delta-theta or beta bands (p values > 0.05, Cohen's $d < 0.42$). These results indicate that MTL stimulation does not affect intraregion phase synchronization.

Effects of MTL stimulation on power in each individual brain region

We examined whether iEEG power differed between the stimulation and nonstimulation trials in each of the brain regions, as this may potentially underlie differences in directed information flow between the MTL and the PFC and PPC. We estimated power in the delta-theta and beta frequency bands (see Materials and Methods) for stimulation and nonstimulation trials and for both the memory encoding and recall periods. Power did not differ between stimulation and nonstimulation trials in the delta-theta or beta frequency bands in any of the brain regions (p values > 0.05, Cohen's $d < 0.68$) (Fig. 6).

Together, these results suggest that the differential directed information flow between the MTL and the PFC and PPC for stimulation and nonstimulation conditions are not driven by differences in the amplitude of iEEG fluctuations.

Effects of MTL stimulation on PAC

Based on previous studies demonstrating PAC between low-frequency delta-theta phase and amplitudes of high-gamma (80-160 Hz) frequency bands (Canolty et al., 2006; Tort et al., 2008), we examined the effects of stimulation on PAC in MTL, MFG, IFG, and dPPC and vPPC. We used the modulation index as an estimate of PAC in individual electrodes in different brain areas (Tort et al., 2008) (see Materials and Methods). This analysis revealed that PAC did not differ between stimulation and nonstimulation trials in any of the brain regions during memory encoding or recall (p values > 0.05, Cohen's $d < 0.80$). This suggests that stimulation of the MTL does not affect PAC in any of the five brain regions.

Discussion

We examined how MTL stimulation alters directed information flow between the MTL and frontoparietal cortical regions implicated in formation and monitoring of episodic memories. We used depth iEEG recordings from the UPENN-RAM cohort in which participants performed a verbal free recall task during concurrent stimulation of MTL neurons. During memory encoding, select MTL electrodes were electrically stimulated at 50 Hz on half the trials (Jacobs et al., 2016; Goyal et al., 2018). Building on our replicable prior findings of frequency-specific interactions between the MTL and PFC (Das and Menon, 2021, 2022), we

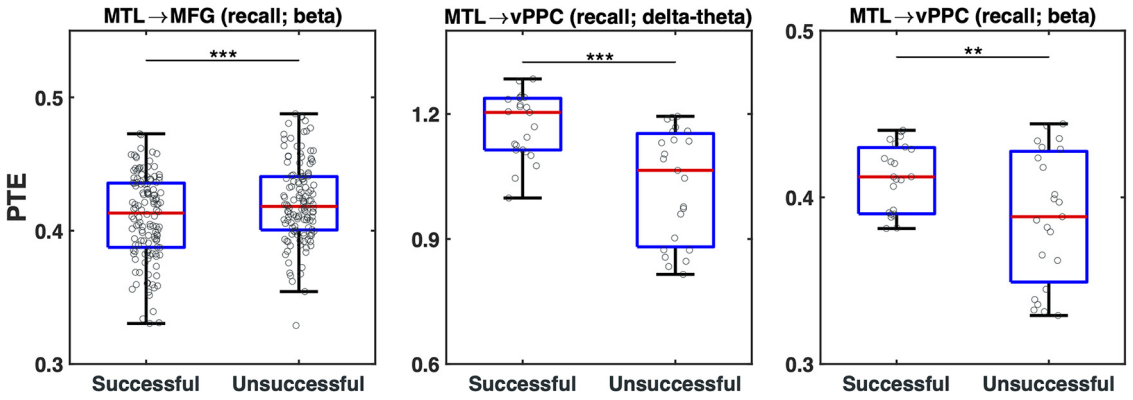

Figure 5. Comparison of directed information flow from the MTL to the MFG and vPPC for successful, compared with unsuccessful, recall during stimulation trials in the memory recall period. MTL→MFG ($n = 132$) information flow was significantly reduced during successful, compared with unsuccessful, recall in the beta band. Moreover, MTL→vPPC ($n = 23$) information flow was significantly higher during successful, compared with unsuccessful, recall in both the δ-theta and β frequency bands. ***$p < 0.001$; **$p < 0.01$; FDR-corrected.

examined how MTL stimulation alters communication between the MTL and MFG subdivision of the PFC (i.e., dorsolateral PFC), during memory encoding, and how this stimulation altered communication during subsequent memory recall. MTL stimulation reduced memory recall (Cohen's effect size = 0.5) and disrupted directed information flow with the PFC. Figure 7 summarizes our key findings.

MTL stimulation decreased MFG→MTL information flow in the delta-theta frequency band during the encoding period. Furthermore, the effects of MTL stimulation carried over from the encoding to the subsequent memory recall period, despite a ~20 s delay period in which there was no external stimulation of the MTL. This process was characterized by decreased top-down MFG→MTL information flow in the beta frequency band. However, there was no difference in top-down PPC→MTL information flow. A direct comparison between the PFC and PPC revealed stronger modulation of top-down influences on the MTL from the PFC, compared with the PPC. Together, these findings demonstrate that MTL stimulation disrupts processing specifically in the PFC in the low-frequency delta-theta range during memory encoding with aftereffects that extend to subsequent recall periods.

MTL stimulation effects on directed MTL→PFC and PFC→MTL information flow during memory encoding

The primary goal of our study was to characterize the effect of MTL stimulation on directed information flow between the MTL and the PFC during verbal episodic memory processing. The MTL and MFG (dorsolateral PFC) play a critical role in human episodic memory encoding (Anderson et al., 2010; Watrous et al., 2013; Ekstrom and Watrous, 2014; Neuner et al., 2014; Gonzalez et al., 2015). However, it is unclear how electrical stimulation of the MTL modulates neural dynamics of the targeted regions and the circuits that link them. Specifically, the effect of stimulation on directed information flow between the MTL and the PFC during episodic memory processing is poorly understood.

Our study builds on previously replicated findings across verbal episodic and spatial memory domains which revealed higher bottom-up MTL→PFC information flow than the reverse, in delta-theta and higher top-down PFC→MTL information flow than the reverse, in the beta frequency bands (Das and Menon, 2021, 2022). We used PTE, which provides a robust and powerful tool for characterizing information flow between brain regions based on phase coupling (Lobier et al., 2014; Hillebrand et al., 2016; M. Y. Wang et al., 2017).

We took an unbiased approach for assigning electrodes to individual anatomically defined brain regions, and we did not select electrodes based on arbitrary task or stimulation-induced activation profiles. Our approach thus allowed us to probe the electrophysiological correlates of the effects of MTL stimulation on directed information flow between the MTL and PFC more generally. We found that MTL stimulation decreased PFC→MTL information flow during the encoding period, in delta-theta band. Notably, these effects were specific to the dorsolateral MFG subdivision of the PFC and were not observed in the more ventral aspects that comprise the IFG.

We conducted control analyses to ensure that the reported effects related to the directed information flow between the MTL and the MFG did not arise solely from brain stimulation causing reorganization of brain circuits. Specifically, we used "resting-state" data from a separate group of participants, also acquired and released as part of the UPENN-RAM public data release (Solomon et al., 2021). Participants were instructed to sit quietly and did not perform any task. Similar to the memory task, in the resting-state condition, bipolar stimulation current between pairs of depth MTL electrodes was applied at 50 Hz. We found that, in contrast to the memory task, neither MTL→MFG nor MFG→MTL directed information flow changed during stimulation, compared with the nonstimulation, trials in the delta-theta frequency band. These results suggest that directed information flow between the MTL and the MFG observed during the memory task are not solely attributable to brain stimulation-induced reorganization of brain circuits, rather they are related to the combined effects of stimulation and memory processing.

MTL stimulation effects on directed MTL→PFC and PFC→MTL information flow during memory recall

Crucially, the effects of MTL stimulation were also detectable in the subsequent recall period which occurred after a delay of 20 s. This finding is consistent with previous human iEEG studies which have observed strong afterdischarge iEEG signals within and outside the MTL during memory retrieval, which occurred tens of seconds after MTL stimulation was applied during the encoding period of an episodic memory task (Halgren et al., 1985; Jun et al., 2020). Moreover, similar to our findings, these afterdischarge effects were linked to memory impairment in these studies (Halgren et al., 1985; Jun et al., 2020). Specifically, we observed decreased MFG→MTL information flow on stimulation, compared

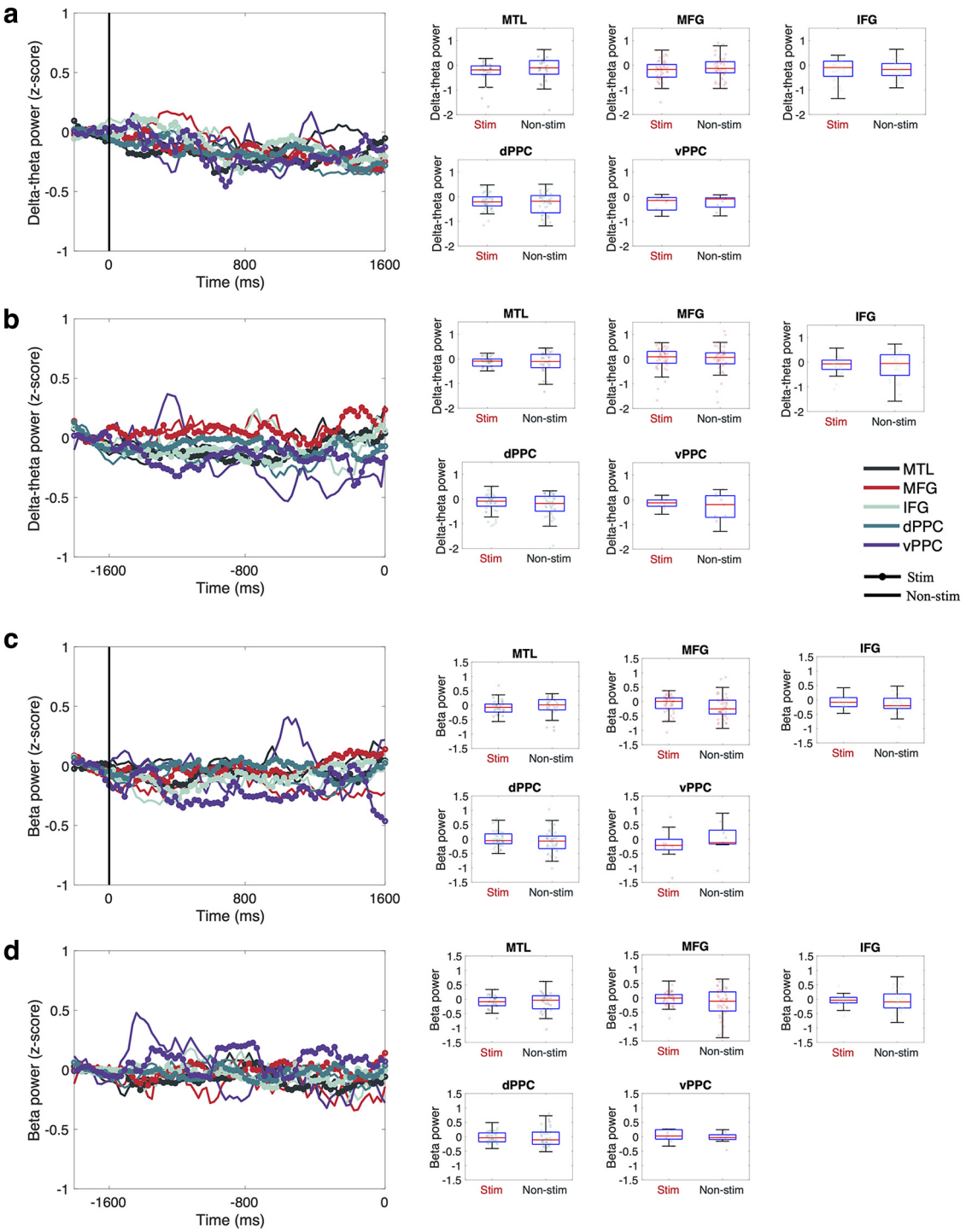

Figure 6. Spectral power in the δ-theta (0.5-8 Hz) and β (12-30 Hz) frequency bands during stimulation compared with nonstimulation trials for the encoding and retrieval periods. ***a***, Spectral power in the δ-theta band during encoding periods. ***b***, Spectral power in the δ-theta band during recall periods. ***c***, Spectral power in the beta band during encoding periods. ***d***, Spectral power in the beta band during recall periods. Zero on the x-axis indicates the onset of word presentation for the encoding periods and the verbal recall of a word during the recall periods.

with nonstimulation, trials in the beta frequency band. Again, this effect was specific to the dorsolateral MFG subdivision of the PFC, which is known to play a prominent role in top-down control of both subcortical and cortical regions involved in memory formation (Brovelli et al., 2004; Engel and Fries, 2010; Spitzer and Haegens, 2017; Stanley et al., 2018). Extending our findings of spectrally resolved top-down influences from the PFC, we found MTL stimulation effects in the beta band but not in the δ–theta frequency band, providing consistent evidence for spectral dissociation associated with the beta frequency band. Theoretical models have pointed to both excitatory and inhibitory mechanisms underlying deep brain stimulation (Vitek, 2002; McIntyre et al., 2004). We did not observe changes in power of iEEG signals in either frequency band, suggesting causal circuit mechanisms arising from phase, rather than amplitude, changes underlie the observed MTL stimulation related changes in information flow.

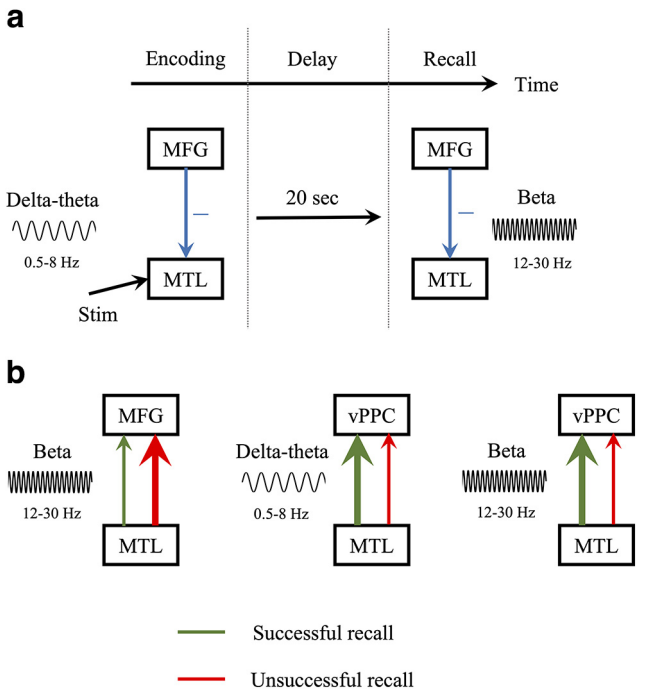

Figure 7. Schematic illustration of key findings related to MTL stimulation. ***a***, Directed information flow on successful trials. MTL stimulation decreased concurrent directed information flow from the MFG subdivision of the PFC to the MTL during memory encoding (δ-theta band). These effects were specific to MFG and were not observed in IFG or dorsal or ventral nodes of PPC. MTL stimulation aftereffects were observed in the subsequent memory recall period >20 s later, characterized by decreased top-down information flow from MFG to MTL (beta band); again, these effects were specific to MFG and were not observed in IFG or dorsal or ventral nodes of the PPC. Blue arrows indicate decrease during stimulation, compared with nonstimulation, trials. ***b***, Comparison of directed information flow during successful versus unsuccessful memory recall. MTL to MFG information flow on stimulation trials was significantly lower for successful, compared with unsuccessful, memory recall (beta band). In contrast, MTL to vPPC information flow was significantly higher for successful, compared with unsuccessful, memory recall (both δ-theta and β bands). Thickness of arrows corresponds to relative strength of information flow, with higher thickness denoting stronger information flow.

LFP studies in monkeys have demonstrated a more prominent role for the dorsal, compared with the ventral, PFC in top-down control in the beta frequency band for processing higher-level abstractions during working memory performance (Wutz et al., 2018). Electrophysiology studies in rodents performing an odor-place associative memory-guided decision task on a T-maze have shown that hippocampal-PFC coherence in the beta frequency band is linked to accurate decisions (Symanski et al., 2022). LFP studies in monkeys performing a paired association learning task have shown that beta oscillations in the MFG encode picture-color association (Tanigawa et al., 2022). fMRI studies in humans have shown that the dorsal MFG is a part of the central executive network which plays an important role in memory processing and complex decision-making (Seeley et al., 2007; Sridharan et al., 2008; Menon and Uddin, 2010). Additionally, MEG and iEEG studies in humans have shown a prominent role of beta for feedback signaling (Michalareas et al., 2016; Hayat et al., 2022). Consistent with our findings, rodent studies have also shown that inhibition of PFC projections to the hippocampus impairs memory recall (Rajasethupathy et al., 2015; Yadav et al., 2022). Reduction in neural signaling from the MFG to the MTL during memory recall may explain why stimulation of the MTL reduces or impairs memory performance (Coleshill et al., 2004; Lacruz et al., 2010; Jacobs et al., 2016; Goyal et al., 2018).

A recent study using 1 Hz repetitive transcranial magnetic stimulation (rTMS) of the MFG found enhancement of verbal memory performance and also showed that this stimulation induced stronger beta power modulation in the posterior areas (van der Plas et al., 2021), suggesting that neuromodulatory effects in the MFG might be the most prominent in the beta frequency band. A meta-analysis of rTMS studies has revealed that 1 Hz rTMS of the MFG usually leads to an enhancement of episodic memory performance, whereas 20 Hz rTMS of the MFG usually leads to a reduction in episodic memory performance (Yeh and Rose, 2019). These results indicate a disruptive effect of beta on MFG neural dynamics at frequencies significantly >1 Hz, including the 50 Hz stimulation frequency used in our study, and may explain the reduction of information flow from the MFG that we observed during the recall periods in this frequency band.

Dissociable effects of MTL stimulation on top-down causal information flow from PFC and PPC

The next goal of our study was to contrast the effects of MTL stimulation on information flow with the PFC and PPC. In addition to the PFC, the PPC also plays an important role in episodic memory (Tulving et al., 1994; Moscovitch et al., 1995; Schacter et al., 1996). PTE analysis revealed that, in contrast to the PFC, there were no differences between stimulation and nonstimulation trials in top-down dPPC→MTL information flow. A direct comparison revealed stronger MTL stimulation-induced modulation of top-down MFG→MTL, compared with dPPC→MTL in the beta frequency band (Fig. 4). Information flow between the MTL and vPPC was unaffected by MTL stimulation, and a direct comparison confirmed stronger MTL stimulation-induced modulation of top-down MFG→MTL, compared with vPPC→MTL in the beta frequency band. This suggests that the dorsolateral MFG subdivision of the PFC is more sensitive to MTL stimulation than PPC regions involved in episodic memory.

Electrophysiology studies in monkeys have shown that the PFC is more sensitive to memory encoding compared with the PPC (Qi et al., 2015; Masse et al., 2017; Murray et al., 2017; Zhou et al., 2021; Dang et al., 2022). Specifically, these studies showed that, compared with the PPC, neurons in the PFC are more responsive (Dang et al., 2022), show more persistent firing rate (Masse et al., 2017), and are more robust to distractors (Qi et al., 2015; Murray et al., 2017; Zhou et al., 2021). Together, these findings suggest that the MFG may play an enhanced role compared with the PPC in memory formation, which may make it a more sensitive target of brain stimulation compared with the PPC in humans (J. X. Wang et al., 2014).

Behavioral specificity of the effects of MTL stimulation

Finally, we examined whether the observed effects of MTL stimulation on information flow between different brain regions reflect cognitive processes related to memory encoding, or whether they are solely attributable to the reorganization of brain circuits from the effects of stimulation. We tested the hypothesis that the information flow between different brain areas would differ between successful and unsuccessful memory trials during stimulation, thus putatively reflecting cognitive processes related to memory processing, rather than effects of stimulation only.

We found that the direction of information flow between the MTL and both the PFC and PPC during memory recall is behaviorally relevant. Results support the hypotheses that causal signaling from the MTL to both regions are associated with memory

recall processes, rather than arising solely from the effects of MTL stimulation-related reorganization of brain circuits. MTL→MFG directed information flow was significantly lower for successful, compared with unsuccessful, memory recall in the beta band. This suggests that the higher causal signaling between the MTL→MFG in the beta band during unsuccessful trials is disruptive during recall.

Crucially, we found that the direction of information flow between the MTL and the vPPC during memory recall was also behaviorally relevant. MTL→vPPC directed information flow was significantly higher for successful, compared with unsuccessful, memory recall in both the delta-theta and beta frequency bands. MTL-vPPC have been previously proposed to form a coherent set of network and interactions within this network have been proposed to play a crucial role in memory processing in humans (Wagner et al., 2005; Ranganath and Ritchey, 2012). Moreover, noninvasive rTMS to the vPPC area is known to be associated with successful associative memory retrieval in humans (J. X. Wang et al., 2014). The increased MTL→vPPC directed information flow that we observed for the successful trials during memory recall is thus consistent with the prominent role of the vPPC for episodic memory retrieval and extends our understanding of directed causal signaling that supports such a role in the human brain.

Together, these results demonstrate that stimulating the MTL has a significant impact on communication between the MTL and the PFC and PPC, which can either enhance or hinder memory recall. Additionally, the results indicate that the direction of information flow in the MTL is not solely because of reorganization of brain circuits caused by stimulation, but rather a combination of stimulation and memory processing.

Limitations

The stimulation paradigm used in the study was applied only at a single frequency (50 Hz) (see Materials and Methods). Previous studies in humans have usually applied direct stimulation at theta and gamma frequencies to modulate memory performance, which are considered to be the endogenous rhythms of the MTL (Eichenbaum, 2017), although these frequencies have had a varied effect on memory performance. Whereas theta frequency stimulation has shown improvement in memory performance (Koubeissi et al., 2013; Lee et al., 2013; Alagapan et al., 2019), stimulation at 50 Hz has shown heterogeneous patterns of memory performance, with some studies suggesting memory enhancement (Suthana et al., 2012; Fell et al., 2013; Inman et al., 2018), while others have found impairment in memory performance (Coleshill et al., 2004; Lacruz et al., 2010; Jacobs et al., 2016; Goyal et al., 2018). Limitations of electrode placement precluded analysis of causal circuit dynamics associated with each hemisphere and distinct subdivisions of the MTL; denser sampling of electrodes in multiple brain regions with a wider range of experimental tasks, and a larger number of participants are needed to further address these limitations. Additionally, studies with memory and resting-state iEEG data acquired in the same participants are needed to confirm that the effects of MTL stimulation reported in our study are not solely attributable to brain stimulation-induced reorganization of brain circuits. Finally, it is not known whether some of the patients may have shown considerable memory dysfunction in formal neuropsychological testing. Future studies with rigorous neuropsychological testing procedures are needed to determine the effect of brain stimulation in patients with different cognitive abilities.

In the present study, participants received stimulation at a range of current amplitudes, starting from 0.25 to 1.5 mA. The choice of the current amplitude values for the cognitive experiments of the participants was the maximum current for each site that could be applied without inducing patient symptoms, epileptiform after discharges, or seizures. Lack of sufficient participants and electrode pairs for each of these current amplitude values did not allow us to study the effects of current amplitude on the information flow between the MTL and the PFC and PPC. Future studies will also need to consider the effects of a range of stimulation frequencies and currents, and electrode sites across MTL subdivisions in gray/white matter to rigorously assess other factors that influence memory performance, monitoring, and directed information flow between the MTL and PFC.

In conclusion, our findings provide novel evidence that MTL stimulation alters directed information flow with the PFC and PPC and that these influences are behaviorally relevant. Stimulating the MTL decreased flow of information from PFC to the MTL during both the encoding and recall periods, with effects lasting for >20 s after end of stimulation. This suppression of top-down PFC to MTL influences was stronger than suppression of PPC to MTL influences. Additionally, the flow of information from MTL to PFC was lower during successful memory recall compared with unsuccessful recall, while the flow of information from the MTL to the vPPC was higher during successful recall. These results show that the effects of MTL stimulation are specific to behavior, region, and direction, that MTL stimulation specifically impairs communication with the PFC, and that causal MTL-vPPC circuits support successful memory recall. Findings further suggest that information theoretic measures based on phase delays may provide a more robust measure of the effects of stimulation than other measures, such as changes in power and PAC. Crucially, our findings demonstrate that suppression of the dorsolateral PFC is a locus of circuit vulnerability induced by MTL stimulation. Findings uncover a mechanism by which human MTL stimulation disrupts both formation and retrieval of recent memories (Halgren et al., 1985). Our findings have implications for translational applications aimed at realizing the promise of brain stimulation-based treatment of memory disorders.

References

Alagapan S, Lustenberger C, Hadar E, Shin HW, Fröhlich F (2019) Low-frequency direct cortical stimulation of left superior frontal gyrus enhances working memory performance. Neuroimage 184:697–706.

Amer T, Davachi L (2022) Neural mechanisms of memory. In: Oxford handbook of human memory (Kahana MJ, Wagner AD, eds). Oxford: Oxford UP.

Amorapanth PX, Widick P, Chatterjee A (2010) The neural basis for spatial relations. J Cogn Neurosci 22:1739–1753.

Andersen RA, Essick GK, Siegel RM (1985) Encoding of spatial location by posterior parietal neurons. Science 230:456–458.

Anderson KL, Rajagovindan R, Ghacibeh GA, Meador KJ, Ding M (2010) Theta oscillations mediate interaction between prefrontal cortex and medial temporal lobe in human memory. Cereb Cortex 20:1604–1612.

Backus AR, Schoffelen JM, Szebényi S, Hanslmayr S, Doeller CF (2016) Hippocampal-prefrontal theta oscillations support memory integration. Curr Biol 26:450–457.

Badre D, Poldrack RA, Paré-Blagoev EJ, Insler RZ, Wagner AD (2005) Dissociable controlled retrieval and generalized selection mechanisms in ventrolateral prefrontal cortex. Neuron 47:907–918.

Badre D, Wagner AD (2007) Left ventrolateral prefrontal cortex and the cognitive control of memory. Neuropsychologia 45:2883–2901.

Barnett L, Seth AK (2014) The MVGC multivariate Granger causality toolbox: a new approach to Granger-causal inference. J Neurosci Methods 223:50–68.

Baumann O, Chan E, Mattingley JB (2012) Distinct neural networks underlie encoding of categorical versus coordinate spatial relations during active navigation. Neuroimage 60:1630–1637.

Brincat SL, Miller EK (2015) Frequency-specific hippocampal-prefrontal interactions during associative learning. Nat Neurosci 18:576–581.

Brovelli A, Ding M, Ledberg A, Chen Y, Nakamura R, Bressler SL (2004) Beta oscillations in a large-scale sensorimotor cortical network: directional influences revealed by Granger causality. Proc Natl Acad Sci USA 101:9849–9854.

Bruns A (2004) Fourier-, Hilbert- and wavelet-based signal analysis: are they really different approaches? J Neurosci Methods 137:321–332.

Buckner RL, Koutstaal W, Schacter DL, Dale AM, Rotte M, Rosen BR (1998) Functional-anatomic study of episodic retrieval: II. Selective averaging of event-related fMRI trials to test the retrieval success hypothesis. Neuroimage 7:163–175.

Burke JF, Zaghloul KA, Jacobs J, Williams RB, Sperling MR, Sharan AD, Kahana MJ (2013) Synchronous and asynchronous theta and gamma activity during episodic memory formation. J Neurosci 33:292–304.

Cabeza R (2008) Role of parietal regions in episodic memory retrieval: the dual attentional processes hypothesis. Neuropsychologia 46:1813–1827.

Cabeza R, Ciaramelli E, Olson IR, Moscovitch M (2008) The parietal cortex and episodic memory: an attentional account. Nat Rev Neurosci 9:613–625.

Cabeza R, Mazuz YS, Stokes J, Kragel JE, Woldorff MG, Ciaramelli E, Olson IR, Moscovitch M (2011) Overlapping parietal activity in memory and perception: evidence for the attention to memory model. J Cogn Neurosci 23:3209–3217.

Cabeza R, Ciaramelli E, Moscovitch M (2012) Cognitive contributions of the ventral parietal cortex: an integrative theoretical account. Trends Cogn Sci 16:338–352.

Canolty RT, Edwards E, Dalal SS, Soltani M, Nagarajan SS, Kirsch HE, Berger MS, Barbaro NM, Knight RT (2006) High gamma power is phase-locked to theta oscillations in human neocortex. Science 313:1626–1628.

Chen LL, Lin LH, Green EJ, Barnes CA, McNaughton BL (1994) Head-direction cells in the rat posterior cortex: I. Anatomical distribution and behavioral modulation. Exp Brain Res 101:8–23.

Chua EF, Ahmed R (2016) Electrical stimulation of the dorsolateral prefrontal cortex improves memory monitoring. Neuropsychologia 85:74–79.

Ciaramelli E, Grady CL, Moscovitch M (2008) Top-down and bottom-up attention to memory: a hypothesis (AtoM) on the role of the posterior parietal cortex in memory retrieval. Neuropsychologia 46:1828–1851.

Ciaramelli E, Burianová H, Vallesi A, Cabeza R, Moscovitch M (2020) Functional interplay between posterior parietal cortex and hippocampus during detection of memory targets and non-targets. Front Neurosci 14:563768.

Clower DM, West RA, Lynch JC, Strick PL (2001) The inferior parietal lobule is the target of output from the superior colliculus, hippocampus, and cerebellum. J Neurosci 21:6283–6291.

Coleshill SG, Binnie CD, Morris RG, Alarcón G, van Emde Boas W, Velis DN, Simmons A, Polkey CE, van Veelen CW, van Rijen PC (2004) Material-specific recognition memory deficits elicited by unilateral hippocampal electrical stimulation. J Neurosci 24:1612–1616.

Crowe DA, Chafee MV, Averbeck BB, Georgopoulos AP (2004) Neural activity in primate parietal area 7a related to spatial analysis of visual mazes. Cereb Cortex 14:23–34.

Cruzado NA, Tiganj Z, Brincat SL, Miller EK, Howard MW (2020) Conjunctive representation of what and when in monkey hippocampus and lateral prefrontal cortex during an associative memory task. Hippocampus 30:1332–1346.

Curtis CE (2006) Prefrontal and parietal contributions to spatial working memory. Neuroscience 139:173–180.

Dang W, Li S, Pu S, Qi XL, Constantinidis C (2022) More prominent nonlinear mixed selectivity in the dorsolateral prefrontal than posterior parietal cortex. eNeuro 9:ENEURO.0517-21.2022.

Das A, Menon V (2020) Spatiotemporal integrity and spontaneous nonlinear dynamic properties of the salience network revealed by human intracranial electrophysiology: a multicohort replication. Cereb Cortex 30:5309–5321.

Das A, Menon V (2021) Asymmetric frequency-specific feedforward and feedback information flow between hippocampus and prefrontal cortex during verbal memory encoding and recall. J Neurosci 41:8427–8440.

Das A, Menon V (2022) Replicable patterns of causal information flow between hippocampus and prefrontal cortex during spatial navigation and spatial-verbal memory formation. Cereb Cortex 32:5343–5361.

Daselaar SM, Prince SE, Dennis NA, Hayes SM, Kim H, Cabeza R (2009) Posterior midline and ventral parietal activity is associated with retrieval success and encoding failure. Front Hum Neurosci 3:13.

Dickerson BC, Eichenbaum H (2010) The episodic memory system: neurocircuitry and disorders. Neuropsychopharmacology 35:86–104.

Dobbins IG, Foley H, Schacter DL, Wagner AD (2002) Executive control during episodic retrieval: multiple prefrontal processes subserve source memory. Neuron 35:989–996.

Eichenbaum H (2017) Prefrontal-hippocampal interactions in episodic memory. Nat Rev Neurosci 18:547–558.

Ekstrom AD, Caplan JB, Ho E, Shattuck K, Fried I, Kahana MJ (2005) Human hippocampal theta activity during virtual navigation. Hippocampus 15:881–889.

Ekstrom AD, Watrous AJ (2014) Multifaceted roles for low-frequency oscillations in bottom-up and top-down processing during navigation and memory. Neuroimage 85:667–677.

Engel AK, Fries P (2010) Beta-band oscillations: signalling the status quo? Curr Opin Neurobiol 20:156–165.

Ezzyat Y, et al. (2018) Closed-loop stimulation of temporal cortex rescues functional networks and improves memory. Nat Commun 9:365.

Fan L, Li H, Zhuo J, Zhang Y, Wang J, Chen L, Yang Z, Chu C, Xie S, Laird AR, Fox PT, Eickhoff SB, Yu C, Jiang T (2016) The Human Brainnetome Atlas: a new brain atlas based on connectional architecture. Cereb Cortex 26:3508–3526.

Fell J, Staresina BP, Do Lam AT, Widman G, Helmstaedter C, Elger CE, Axmacher N (2013) Memory modulation by weak synchronous deep brain stimulation: a pilot study. Brain Stimul 6:270–273.

Fernandez G, Hufnagel A, Helmstaedter C, Zentner J, Elger CE (1996) Memory function during low intensity hippocampal electrical stimulation in patients with temporal lobe epilepsy. Eur J Neurol 3:335–344.

Gonzalez A, Hutchinson JB, Uncapher MR, Chen J, LaRocque KF, Foster BL, Rangarajan V, Parvizi J, Wagner AD (2015) Electrocorticography reveals the temporal dynamics of posterior parietal cortical activity during recognition memory decisions. Proc Natl Acad Sci USA 112:11066–11071.

Goyal A, Miller J, Watrous AJ, Lee SA, Coffey T, Sperling MR, Sharan A, Worrell G, Berry B, Lega B, Jobst BC, Davis KA, Inman C, Sheth SA, Wanda PA, Ezzyat Y, Das SR, Stein J, Gorniak R, Jacobs J (2018) Electrical stimulation in hippocampus and entorhinal cortex impairs spatial and temporal memory. J Neurosci 38:4471–4481.

Grover S, Nguyen JA, Reinhart RM (2021) Synchronizing brain rhythms to improve cognition. Annu Rev Med 72:29–43.

Guitart-Masip M, Barnes GR, Horner A, Bauer M, Dolan RJ, Duzel E (2013) Synchronization of medial temporal lobe and prefrontal rhythms in human decision making. J Neurosci 33:442–451.

Gurd JM, Amunts K, Weiss PH, Zafiris O, Zilles K, Marshall JC, Fink GR (2002) Posterior parietal cortex is implicated in continuous switching between verbal fluency tasks: an fMRI study with clinical implications. Brain 125:1024–1038.

Halgren E, Wilson CL, Stapleton JM (1985) Human medial temporal-lobe stimulation disrupts both formation and retrieval of recent memories. Brain Cogn 4:287–295.

Hansen N, Chaieb L, Derner M, Hampel KG, Elger CE, Surges R, Staresina B, Axmacher N, Fell J (2018) Memory encoding-related anterior hippocampal potentials are modulated by deep brain stimulation of the entorhinal area. Hippocampus 28:12–17.

Hasegawa I, Hayashi T, Miyashita Y (1999) Memory retrieval under the control of the prefrontal cortex. Ann Med 31:380–387.

Hayat H, Marmelshtein A, Krom AJ, Sela Y, Tankus A, Strauss I, Fahoum F, Fried I, Nir Y (2022) Reduced neural feedback signaling despite robust neuron and gamma auditory responses during human sleep. Nat Neurosci 25:935–943.

Herweg NA, Solomon EA, Kahana MJ (2020) Theta oscillations in human memory. Trends Cogn Sci 24:208–227.

Hillebrand A, Tewarie P, van Dellen E, Yu M, Carbo EW, Douw L, Gouw AA, van Straaten EC, Stam CJ (2016) Direction of information flow in large-scale resting-state networks is frequency-dependent. Proc Natl Acad Sci USA 113:3867–3872.

Huang Y, Keller C (2022) How can I investigate causal brain networks with iEEG? In: Intracranial EEG for cognitive neuroscientists (Axmacher N, ed). New York: Springer.

Husain M, Nachev P (2007) Space and the parietal cortex. Trends Cogn Sci 11:30–36.

Hutchinson JB, Uncapher MR, Wagner AD (2009) Posterior parietal cortex and episodic retrieval: convergent and divergent effects of attention and memory. Learn Mem 16:343–356.

Inman CS, Manns JR, Bijanki KR, Bass DI, Hamann S, Drane DL, Fasano RE, Kovach CK, Gross RE, Willie JT (2018) Direct electrical stimulation of the amygdala enhances declarative memory in humans. Proc Natl Acad Sci USA 115:98–103.

Insausti R, Muñoz M (2001) Cortical projections of the non-entorhinal hippocampal formation in the cynomolgus monkey (*Macaca fascicularis*). Eur J Neurosci 14:435–451.

Jackson JB, Feredoes E, Rich AN, Lindner M, Woolgar A (2021) Concurrent neuroimaging and neurostimulation reveals a causal role for dlPFC in coding of task-relevant information. Commun Biol 4:588.

Jacobs J, Miller J, Lee SA, Coffey T, Watrous AJ, Sperling MR, Sharan A, Worrell G, Berry B, Lega B, Jobst BC, Davis K, Gross RE, Sheth SA, Ezzyat Y, Das SR, Stein J, Gorniak R, Kahana MJ, Rizzuto DS (2016) Direct electrical stimulation of the human entorhinal region and hippocampus impairs memory. Neuron 92:983–990.

Jun S, Lee SA, Kim JS, Jeong W, Chung CK (2020) Task-dependent effects of intracranial hippocampal stimulation on human memory and hippocampal theta power. Brain Stimul 13:603–613.

Kahana MJ (2006) The cognitive correlates of human brain oscillations. J Neurosci 26:1669–1672.

Kim K, Ekstrom AD, Tandon N (2016) A network approach for modulating memory processes via direct and indirect brain stimulation: toward a causal approach for the neural basis of memory. Neurobiol Learn Mem 134:162–177.

Konishi S, Wheeler ME, Donaldson DI, Buckner RL (2000) Neural correlates of episodic retrieval success. Neuroimage 12:276–286.

Koubeissi MZ, Kahriman E, Syed TU, Miller J, Durand DM (2013) Low-frequency electrical stimulation of a fiber tract in temporal lobe epilepsy. Ann Neurol 74:223–231.

Kucewicz MT, Cimbalnik J, Matsumoto JY, Brinkmann BH, Bower MR, Vasoli V, Sulc V, Meyer F, Marsh WR, Stead SM, Worrell GA (2014) High frequency oscillations are associated with cognitive processing in human recognition memory. Brain 137:2231–2244.

Kucewicz MT, Berry BM, Kremen V, Miller LR, Khadjevand F, Ezzyat Y, Stein JM, Wanda P, Sperling MR, Gorniak R, Davis KA, Jobst BC, Gross RE, Lega B, Stead SM, Rizzuto DS, Kahana MJ, Worrell GA (2018a) Electrical stimulation modulates high γ activity and human memory performance. eNeuro 5:ENEURO.0369-17.2018.

Kucewicz MT, Berry BM, Miller LR, Khadjevand F, Ezzyat Y, Stein JM, Kremen V, Brinkmann BH, Wanda P, Sperling MR, Gorniak R, Davis KA, Jobst BC, Gross RE, Lega B, Van Gompel J, Stead SM, Rizzuto DS, Kahana MJ, Worrell GA (2018b) Evidence for verbal memory enhancement with electrical brain stimulation in the lateral temporal cortex. Brain 141:971–978.

Kumaran D, Summerfield JJ, Hassabis D, Maguire EA (2009) Tracking the emergence of conceptual knowledge during human decision making. Neuron 63:889–901.

Kuznetsova A, Brockhoff PB, Christensen RH (2017) lmerTest package: tests in linear mixed effects models. J Stat Soft 82:1–26.

Kwon H, Kronemer SI, Christison-Lagay KL, Khalaf A, Li J, Ding JZ, Freedman NC, Blumenfeld H (2021) Early cortical signals in visual stimulus detection. Neuroimage 244:118608.

Lachaux JP, Rodriguez E, Martinerie J, Varela FJ (1999) Measuring phase synchrony in brain signals. Hum Brain Mapp 8:194–208.

Lachaux JP, Axmacher N, Mormann F, Halgren E, Crone NE (2012) High-frequency neural activity and human cognition: past, present and possible future of intracranial EEG research. Prog Neurobiol 98:279–301.

Lacruz ME, Valentín A, Seoane JJ, Morris RG, Selway RP, Alarcón G (2010) Single pulse electrical stimulation of the hippocampus is sufficient to impair human episodic memory. Neuroscience 170:623–632.

Lee DJ, Gurkoff GG, Izadi A, Berman RF, Ekstrom AD, Muizelaar JP, Lyeth BG, Shahlaie K (2013) Medial septal nucleus theta frequency deep brain stimulation improves spatial working memory after traumatic brain injury. J Neurotrauma 30:131–139.

Lobier M, Siebenhühner F, Palva S, Matias PJ (2014) Phase transfer entropy: a novel phase-based measure for directed connectivity in networks coupled by oscillatory interactions. Neuroimage 85:853–872.

Long NM, Burke JF, Kahana MJ (2014) Subsequent memory effect in intracranial and scalp EEG. Neuroimage 84:488–494.

Masse NY, Hodnefield JM, Freedman DJ (2017) Mnemonic encoding and cortical organization in parietal and prefrontal cortices. J Neurosci 37:6098–6112.

McIntyre CC, Grill WM, Sherman DL, Thakor NV (2004) Cellular effects of deep brain stimulation: model-based analysis of activation and inhibition. J Neurophysiol 91:1457–1469.

McNaughton BL, Mizumori SJ, Barnes CA, Leonard BJ, Marquis M, Green EJ (1994) Cortical representation of motion during unrestrained spatial navigation in the rat. Cereb Cortex 4:27–39.

Menon V, Uddin LQ (2010) Saliency, switching, attention and control: a network model of insula function. Brain Struct Funct 214:655–667.

Menon V, Freeman WJ, Cutillo BA, Desmond JE, Ward MF, Bressler SL, Laxer KD, Barbaro N, Gevins AS (1996) Spatio-temporal correlations in human gamma band electrocorticograms. Electroencephalogr Clin Neurophysiol 98:89–102.

Mercier MR, et al. (2022) Advances in human intracranial electroencephalography research, guidelines and good practices. Neuroimage 260: 119438.

Merkow MB, Burke JF, Ramayya AG, Sharan AD, Sperling MR, Kahana MJ (2017) Stimulation of the human medial temporal lobe between learning and recall selectively enhances forgetting. Brain Stimul 10:645–650.

Meyer-Lindenberg AS, Olsen RK, Kohn PD, Brown T, Egan MF, Weinberger DR, Berman KF (2005) Regionally specific disturbance of dorsolateral prefrontal-hippocampal functional connectivity in schizophrenia. Arch Gen Psychiatry 62:379–386.

Michalareas G, Vezoli J, van Pelt S, Schoffelen JM, Kennedy H, Fries P (2016) Alpha-beta and gamma rhythms subserve feedback and feedforward influences among human visual cortical areas. Neuron 89:384–397.

Miyamoto K, Osada T, Adachi Y, Matsui T, Kimura HM, Miyashita Y (2013) Functional differentiation of memory retrieval network in macaque posterior parietal cortex. Neuron 77:787–799.

Mohan UR, Watrous AJ, Miller JF, Lega BC, Sperling MR, Worrell GA, Gross RE, Zaghloul KA, Jobst BC, Davis KA, Sheth SA, Stein JM, Das SR, Gorniak R, Wanda PA, Rizzuto DS, Kahana MJ, Jacobs J (2020) The effects of direct brain stimulation in humans depend on frequency, amplitude, and white-matter proximity. Brain Stimul 13:1183–1195.

Moscovitch C, Kapur S, Köhler S, Houle S (1995) Distinct neural correlates of visual long-term memory for spatial location and object identity: a positron emission tomography study in humans. Proc Natl Acad Sci USA 92:3721–3725.

Moscovitch M, Cabeza R, Winocur G, Nadel L (2016) Episodic memory and beyond: the hippocampus and neocortex in transformation. Annu Rev Psychol 67:105–134.

Murray JD, Jaramillo J, Wang XJ (2017) Working memory and decision-making in a frontoparietal circuit model. J Neurosci 37:12167–12186.

Neuner I, Arrubla J, Werner CJ, Hitz K, Boers F, Kawohl W, Shah NJ (2014) The default mode network and EEG regional spectral power: a simultaneous fMRI-EEG study. PLoS One 9:e88214.

Nitz DA (2006) Tracking route progression in the posterior parietal cortex. Neuron 49:747–756.

Paulk AC, Zelmann R, Crocker B, Widge AS, Dougherty DD, Eskandar EN, Weisholtz DS, Richardson RM, Cosgrove GR, Williams ZM, Cash SS (2022) Local and distant cortical responses to single pulse intracranial stimulation in the human brain are differentially modulated by specific stimulation parameters. Brain Stimul 15:491–508.

Peterson RA, Cavanaugh JE (2018) Ordered quantile normalization: a semiparametric transformation built for the cross-validation era. J Appl Stat 82:2312–2327.

Preston AR, Eichenbaum H (2013) Interplay of hippocampus and prefrontal cortex in memory. Curr Biol 23:R764–773.

Qi XL, Elworthy AC, Lambert BC, Constantinidis C (2015) Representation of remembered stimuli and task information in the monkey dorsolateral prefrontal and posterior parietal cortex. J Neurophysiol 113:44–57.

Qin S, Cho S, Chen T, Rosenberg-Lee M, Geary DC, Menon V (2014) Hippocampal-neocortical functional reorganization underlies children's cognitive development. Nat Neurosci 17:1263–1269.

Rajasethupathy P, Sankaran S, Marshel JH, Kim CK, Ferenczi E, Lee SY, Berndt A, Ramakrishnan C, Jaffe A, Lo M, Liston C, Deisseroth K (2015)

Projections from neocortex mediate top-down control of memory retrieval. Nature 526:653–659.
Ramirez-Zamora A, et al. (2020) Proceedings of the Seventh Annual Deep Brain Stimulation Think Tank: Advances in Neurophysiology, Adaptive DBS, Virtual Reality, Neuroethics and Technology. Front Hum Neurosci 14:54.
Ranganath C, Ritchey M (2012) Two cortical systems for memory-guided behaviour. Nat Rev Neurosci 13:713–726.
Rockland KS, Van Hoesen GW (1999) Some temporal and parietal cortical connections converge in CA1 of the primate hippocampus. Cereb Cortex 9:232–237.
Rolls ET (2018) The storage and recall of memories in the hippocampo-cortical system. Cell Tissue Res 373:577–604.
Rolls ET (2019) The cingulate cortex and limbic systems for action, emotion, and memory. Handb Clin Neurol 166:23–37.
Rossini PM, Rossi S (2007) Transcranial magnetic stimulation: diagnostic, therapeutic, and research potential. Neurology 68:484–488.
Rugg MD (2022) Frontoparietal contributions to retrieval. In: Oxford handbook of human memory (Kahana MJ, Wagner AD, eds). Oxford: Oxford UP.
Rugg MD, Vilberg KL (2013) Brain networks underlying episodic memory retrieval. Curr Opin Neurobiol 23:255–260.
Rutishauser U, Reddy L, Mormann F, Sarnthein J (2021) The architecture of human memory: insights from human single-neuron recordings. J Neurosci 41:883–890.
Schacter DL, Alpert NM, Savage CR, Rauch SL, Albert MS (1996) Conscious recollection and the human hippocampal formation: evidence from positron emission tomography. Proc Natl Acad Sci USA 93:321–325.
Seeley WW, Menon V, Schatzberg AF, Keller J, Glover GH, Kenna H, Reiss AL, Greicius MD (2007) Dissociable intrinsic connectivity networks for salience processing and executive control. J Neurosci 27:2349–2356.
Simons JS, Spiers HJ (2003) Prefrontal and medial temporal lobe interactions in long-term memory. Nat Rev Neurosci 4:637–648.
Solomon EA, Kragel JE, Sperling MR, Sharan A, Worrell G, Kucewicz M, Inman CS, Lega B, Davis KA, Stein JM, Jobst BC, Zaghloul KA, Sheth SA, Rizzuto DS, Kahana MJ (2017) Widespread theta synchrony and high-frequency desynchronization underlies enhanced cognition. Nat Commun 8:1704.
Solomon EA, Stein JM, Das S, Gorniak R, Sperling MR, Worrell G, Inman CS, Tan RJ, Jobst BC, Rizzuto DS, Kahana MJ (2019) Dynamic theta networks in the human medial temporal lobe support episodic memory. Curr Biol 29:1100–1111.e4.
Solomon EA, Sperling MR, Sharan AD, Wanda PA, Levy DF, Lyalenko A, Pedisich I, Rizzuto DS, Kahana MJ (2021) Theta-burst stimulation entrains frequency-specific oscillatory responses. Brain Stimul 14:1271–1284.
Spaak E, de Lange FP (2020) Hippocampal and prefrontal theta-band mechanisms underpin implicit spatial context learning. J Neurosci 40:191–202.
Spitzer B, Haegens S (2017) Beyond the status quo: a role for beta oscillations in endogenous content (re)activation. eNeuro 4:ENEURO.0170-17.2017.
Sridharan D, Levitin DJ, Menon V (2008) A critical role for the right fronto-insular cortex in switching between central-executive and default-mode networks. Proc Natl Acad Sci USA 105:12569–12574.
Stanley DA, Roy JE, Aoi MC, Kopell NJ, Miller EK (2018) Low-beta oscillations turn up the gain during category judgments. Cereb Cortex 28:116–130.
Suthana N, Haneef Z, Stern J, Mukamel R, Behnke E, Knowlton B, Fried I (2012) Memory enhancement and deep-brain stimulation of the entorhinal area. N Engl J Med 366:502–510.
Symanski CA, Bladon JH, Kullberg ET, Miller P, Jadhav SP (2022) Rhythmic coordination and ensemble dynamics in the hippocampal-prefrontal network during odor-place associative memory and decision making. Elife 11:e79545.
Tanigawa H, Majima K, Takei R, Kawasaki K, Sawahata H, Nakahara K, Iijima A, Suzuki T, Kamitani Y, Hasegawa I (2022) Decoding distributed oscillatory signals driven by memory and perception in the prefrontal cortex. Cell Rep 39:110676.
Tort AB, Kramer MA, Thorn C, Gibson DJ, Kubota Y, Graybiel AM, Kopell NJ (2008) Dynamic cross-frequency couplings of local field potential oscillations in rat striatum and hippocampus during performance of a T-maze task. Proc Natl Acad Sci USA 105:20517–20522.
Tulving E, Kapur S, Markowitsch HJ, Craik FI, Habib R, Houle S (1994) Neuroanatomical correlates of retrieval in episodic memory: auditory sentence recognition. Proc Natl Acad Sci USA 91:2012–2015.
Uhlhaas PJ, Singer W (2012) Neuronal dynamics and neuropsychiatric disorders: toward a translational paradigm for dysfunctional large-scale networks. Neuron 75:963–980.
Uncapher MR, Wagner AD (2009) Posterior parietal cortex and episodic encoding: insights from fMRI subsequent memory effects and dual-attention theory. Neurobiol Learn Mem 91:139–154.
van der Plas M, Braun V, Stauch BJ, Hanslmayr S (2021) Stimulation of the left dorsolateral prefrontal cortex with slow rTMS enhances verbal memory formation. PLoS Biol 19:e3001363.
van Kesteren MT, Fernández G, Norris DG, Hermans EJ (2010) Persistent schema-dependent hippocampal-neocortical connectivity during memory encoding and postencoding rest in humans. Proc Natl Acad Sci USA 107:7550–7555.
Vincent JL, Snyder AZ, Fox MD, Shannon BJ, Andrews JR, Raichle ME, Buckner RL (2006) Coherent spontaneous activity identifies a hippocampal-parietal memory network. J Neurophysiol 96:3517–3531.
Vitek JL (2002) Mechanisms of deep brain stimulation: excitation or inhibition. Mov Disord 17[Suppl 3]:S69–S72.
Vogt BA, Pandya DN (1987) Cingulate cortex of the rhesus monkey: II. Cortical afferents. J Comp Neurol 262:271–289.
Wagner AD, Paré-Blagoev EJ, Clark J, Poldrack RA (2001) Recovering meaning: left prefrontal cortex guides controlled semantic retrieval. Neuron 31:329–338.
Wagner AD, Shannon BJ, Kahn I, Buckner RL (2005) Parietal lobe contributions to episodic memory retrieval. Trends Cogn Sci 9:445–453.
Wang JX, Rogers LM, Gross EZ, Ryals AJ, Dokucu ME, Brandstatt KL, Hermiller MS, Voss JL (2014) Targeted enhancement of cortical-hippocampal brain networks and associative memory. Science 345:1054–1057.
Wang MY, Wang J, Zhou J, Guan YG, Zhai F, Liu CQ, Xu FF, Han YX, Yan ZF, Luan GM (2017) Identification of the epileptogenic zone of temporal lobe epilepsy from stereo-electroencephalography signals: a phase transfer entropy and graph theory approach. Neuroimage Clin 16:184–195.
Watrous AJ, Tandon N, Conner CR, Pieters T, Ekstrom AD (2013) Frequency-specific network connectivity increases underlie accurate spatiotemporal memory retrieval. Nat Neurosci 16:349–356.
Wutz A, Loonis R, Roy JE, Donoghue JA, Miller EK (2018) Different levels of category abstraction by different dynamics in different prefrontal areas. Neuron 97:716–726.e8.
Yadav N, Noble C, Niemeyer JE, Terceros A, Victor J, Liston C, Rajasethupathy P (2022) Prefrontal feature representations drive memory recall. Nature 608:153–160.
Yeh N, Rose NS (2019) How can transcranial magnetic stimulation be used to modulate episodic memory? A systematic review and meta-analysis. Front Psychol 10:993.
Zhang W, Guo L, Liu D (2022) Concurrent interactions between prefrontal cortex and hippocampus during a spatial working memory task. Brain Struct Funct 227:1735–1755.
Zhou Y, Rosen MC, Swaminathan SK, Masse NY, Zhu O, Freedman DJ (2021) Distributed functions of prefrontal and parietal cortices during sequential categorical decisions. Elife 10:e58782.